AWARD NUMBER: W81XWH-16-1-0325

TITLE: Inhibition of Chondrocyte Hypertrophy of Osteoarthritis by Disruptor Peptide

PRINCIPAL INVESTIGATOR: Bin Wang

CONTRACTING ORGANIZATION: Thomas Jefferson University
Philadelphia, PA 19107-5116

REPORT DATE: April 2019

TYPE OF REPORT: Final

PREPARED FOR: U.S. Army Medical Research and Materiel Command
Fort Detrick, Maryland 21702-5012

DISTRIBUTION STATEMENT: Approved for Public Release;
Distribution Unlimited

The views, opinions and/or findings contained in this report are those of the author(s) and should not be construed as an official Department of the Army position, policy or decision unless so designated by other documentation.

REPORT DOCUMENTATION PAGE

Form Approved
OMB No. 0704-0188

Public reporting burden for this collection of information is estimated to average 1 hour per response, including the time for reviewing instructions, searching existing data sources, gathering and maintaining the data needed, and completing and reviewing this collection of information. Send comments regarding this burden estimate or any other aspect of this collection of information, including suggestions for reducing this burden to Department of Defense, Washington Headquarters Services, Directorate for Information Operations and Reports (0704-0188), 1215 Jefferson Davis Highway, Suite 1204, Arlington, VA 22202-4302. Respondents should be aware that notwithstanding any other provision of law, no person shall be subject to any penalty for failing to comply with a collection of information if it does not display a currently valid OMB control number. **PLEASE DO NOT RETURN YOUR FORM TO THE ABOVE ADDRESS.**

1. REPORT DATE	**2. REPORT TYPE**	**3. DATES COVERED**
APRIL 2019	FINAL	1 Jul 2016- 31 Dec 2018

4. TITLE AND SUBTITLE

Inhibition of Chondrocyte Hypertrophy of Osteoarthritis by Disruptor Peptide

5a. CONTRACT NUMBER

5b. GRANT NUMBER
W81XWH-16-1-0325

5c. PROGRAM ELEMENT NUMBER

6. AUTHOR(S)
Bin Wang

E-Mail: bin.wang@jefferson.edu

5d. PROJECT NUMBER

5e. TASK NUMBER

5f. WORK UNIT NUMBER

7. PERFORMING ORGANIZATION NAME(S) AND ADDRESS(ES)
Thomas Jefferson University, 1020 Locust Street, Philadelphia, PA 19107-5116

8. PERFORMING ORGANIZATION REPORT NUMBER

9. SPONSORING / MONITORING AGENCY NAME(S) AND ADDRESS(ES)

U.S. Army Medical Research and Materiel Command
Fort Detrick, Maryland 21702-5012

10. SPONSOR/MONITOR'S ACRONYM(S)

11. SPONSOR/MONITOR'S REPORT NUMBER(S)

12. DISTRIBUTION / AVAILABILITY STATEMENT

Approved for Public Release; Distribution Unlimited

13. SUPPLEMENTARY NOTES

14. ABSTRACT

The goal of this research project is to characterize how disruptor peptide blocks beta-catenin interaction with PTH receptor, and inhibits chondrocyte hypertrophy in vitro and in vivo. We designed a disruptor peptide corresponding to the carboxyl-terminal region of PTH receptor, and found this disruptor peptide inhibited beta-catenin binding to PTH receptor by GST-pull down assay. We also confirmed that disruptor peptide conjugated to penetratin can enter cells. Importantly, disruptor peptide reversed the beta-catenin-mediated PTH receptor signaling switch by increasing Gs/cAMP signaling and inhibiting Gq/PLC activation in wild-type and beta-catenin knockout cells by using CRISPR/Cas9 genome-editing technology. In addition, the disruptor peptide enhanced PTHrP stimulated chondrogenesis and promoted PTHrP-inhibited chondrocyte hypertrophy. Furthermore, in mouse osteoarthritis model surgically induced by destabilization of the medial meniscus, articular-injection of PTHrP inhibited both type X collagen (hypertrophic marker) and matrix metalloproteinase 13 (catabolic enzyme). These data suggest that the disruptor peptide favors the therapeutic signaling arm and improves the ability of PTHrP to inhibit cartilage degeneration and treat/prevent osteoarthritis.

15. SUBJECT TERMS

Osteoarthritis**;** Parathyroid hormone-related protein; PTH receptor; Beta-catenin; Chondrocyte hypertrophy

16. SECURITY CLASSIFICATION OF:			**17. LIMITATION OF ABSTRACT**	**18. NUMBER OF PAGES**	**19a. NAME OF RESPONSIBLE PERSON**
a. REPORT	**b. ABSTRACT**	**c. THIS PAGE**			USAMRMC
Unclassified	Unclassified	Unclassified	Unclassified	31	**19b. TELEPHONE NUMBER** *(include area code)*

Table of Contents

Page

1. INTRODUCTION:

Cartilage pathology in osteoarthritis (OA) is associated with extracellular matrix collagen destruction, which is accompanied by phenotypic changes in articular chondrocytes. Chondrocyte hypertrophy-like changes have been well known in both human OA and experimental OA, which are characterized by expression of type X collagen (Col X) and matrix metalloproteinase 13 (MMP13), suggesting the hypertrophic program is activated in OA conditions. The growing evidence indicates that inhibition of the hypertrophic differentiation is able to attenuate the severity of cartilage lesions in mouse OA models. These findings offer new approaches for the treatment of OA by targeting the chondrocyte phenotype to reduce its hypertrophic differentiation. The application of a disruptor peptide to interfere with protein-protein interaction represents a novel therapeutic strategy for inhibition of chondrocyte hypertrophy and treatment/prevention of OA. The purpose of our proposal is to design and develop a novel disruptor peptide and test its efficacy on inhibiting chondrocyte hypertrophy in relevant cellular and in vivo OA models, thus accomplishing most pre-clinical goals necessary for ultimate human subject testing.

2. KEYWORDS:

Osteoarthritis

Parathyroid hormone-related protein

PTH receptor

Beta-catenin

Cell signaling

Chondrocyte hypertrophy

Destabilization of the medial meniscus

3. ACCOMPLISHMENTS:

What were the major goals of the project?

The goal of this research plan is to characterize how disruptor peptide blocks beta-catenin interaction with PTH receptor, inhibits chondrocyte hypertrophy in vitro and in vivo.

What was accomplished under these goals?

The grant project entitled “Inhibition of chondrocyte hypertrophy of osteoarthritis by disruptor peptide” started from July 1, 2016 and ended on December 31, 2018. We completed the work according to the time line in this Discovery Award. We designed a disruptor peptide to block the interaction of PTH receptor with beta-catenin and tested its efficacy on inhibiting chondrocyte hypertrophy in relevant cellular and in vivo osteoarthritis models. Our project established the proof of concept that targeting the inhibition of chondrocyte hypertrophy of osteoarthritis by a disruptor peptide renders PTHrP more effective in prevention/treatment of osteoarthritis.

3.1. Major activities.

The application of disruptor peptide to target the β-catenin interaction with PTH receptor may represent a novel therapeutic strategy for the inhibition of chondrocyte hypertrophy and treatment/prevention of OA.

3.2. Specific objectives

Aim 1 will develop and characterize a disruptor peptide specifically blocks the interaction of beta-catenin with PTH receptor and inhibits the pathogenic beta-catenin-mediated PTH receptor signaling switch. In Aim 2, we will define the role of disruptor peptide in inhibiting chondrocyte differentiation in cells and a mouse DMM (destabilization of the medial meniscus) model.

3.3. Significant results

a. Design a disruptor peptide corresponding to the carboxyl-terminal region of PTH receptor (PTH1R).

Previous findings show that deletion of 5 and 10 amino acids from the carboxyl-terminus of PTH1R residues (589–593 and 584–593) abolished the binding of β-catenin to PTH1R, whereas a deletion of up to the last 4 amino acids in the carboxyl-tail (ETVM), which are PDZ protein NHERF1 and 2 binding sites, did not affect this binding. Mutagenesis analysis of this region identified the critical binding sites of the β-catenin protein to be W589, L585, and L584 of PTH1R. The last 10 amino acids in the carboxyl-tail of human PTH1R are identical to those in rat/mouse PTH1R. Therefore, we propose that the carboxyl-terminal region of 6 amino acids is the β-catenin recognition motif in PTHR. The disruptor peptide and control disruptor peptide were synthesized by PEPTIDE 2.0 (Chantilly, VA).

b. Inhibition of β-catenin binding to PTH1R by GST-pull down assay by disruptor peptide

We generated His-tagged β-catenin and GST-tagged PTH1R proteins. His-β-catenin protein (500 nM) and 500 nM GST-PTH1R were incubated in the presence of different concentrations (0~100 μM) of carboxyl-terminal six-amino-acid disruptor peptide (Dis-pep) or its control peptide (Ctr-pep), which does not interact with β-catenin, in pull-down buffer. Total lysates and immunoprecipitated proteins were analyzed by SDS-polyacrylamide gels and the band intensity for β-catenin and GST-PTH1R was quantified using the Licor Odyssey system. The GST-pull down data showed that the disruptor peptide concentration-dependently inhibited β-catenin binding to PTH1R (**Figure 1**).

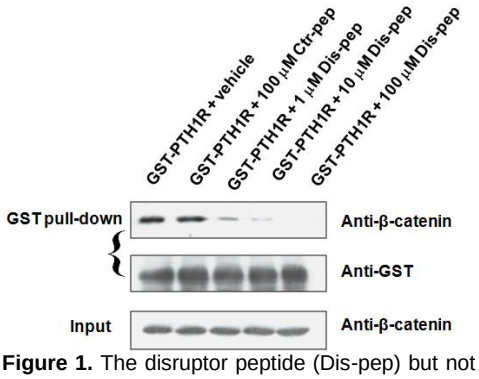

Figure 1. The disruptor peptide (Dis-pep) but not its control peptide (Ctr-pep) inhibits the interaction of PTH receptor (PTH1R) with β-catenin.

c. Disruptor peptide enters cells.

Cellular delivery of peptides is facilitated by peptide conjugation with the carrier, cell-penetrating peptides. To assess disruptor peptide permeability into cells, the effects of disruptor peptide conjugated to penetratin (Pen), which can transport peptide into live cells and animals. To confirm the peptide directly enters cells, we generated the disruptor peptides conjugated with green fluorescent protein (GFP) and/or Pen. Primary chondrocytes were treated with 10 μM of disruptor peptides conjugated with GFP and/or Pen for 2h. The peptides in culture medium were then fully washed with PBS and live cells were visualized using confocal microscopy. Disruptor peptide conjugated with GFP and Pen successfully entered cells (**Figure 2)**.

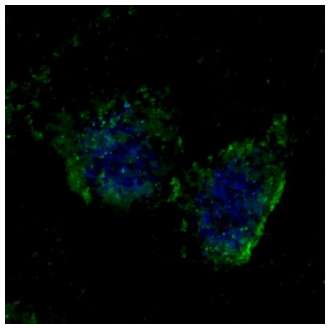

Figure 2. GFP tagged Pen-Dis-pep enters chondrocytes. Nuclear staining was shown in blue.

d. Disruptor peptide reverses the β-catenin-mediated PTH receptor signaling switch in chondrocytes.

Mouse primary rib chondrocytes express both β-catenin and PTH receptor. Cellular delivery of peptides is facilitated by peptide conjugation with the carrier, cell-penetrating peptides. To assess disruptor peptide (6-cdp) permeability into cells, the effects of the disruptor peptide conjugated to: 1) penetratin (Pen); 2) nine arginine residues (9R), or 3) transactivator of transcription (TAT), were compared. Primary chondrocytes were pretreated with 10 μM Pen-6-cdp, 9R-6-cdp, TAT-6-cdp, 6-cdp, Pen, 9R, or TAT for 2 h. cAMP formation induced by 10 nM human PTHrP(1-34) (hereafter referred to as PTHrP) (Bachem, Torrance, CA) for 15 min in the presence of phosphodiesterase inhibitor 3-isobutyl-1-methylxanthine (1 mM) was measured using the cyclic AMP direct EIA kit (Arbor assays, Ann Arbor, MI). **Figure 3A** data demonstrated that the 6-cdp itself, Pen and 9R had no effect on PTHrP-induced cAMP formation. However, the stimulatory effect of PTHrP together with Pen-6-cdp was higher than that of 9R-6cdp and TAT-6cdp. Therefore, the 6-cdp conjugated with Pen was used in the following experiments. As expected, Pen-6-cdp concentration-dependently increased 10 nM PTHrP-induced cAMP formation (**Figure 3B**), while control peptide (Pen-ctr-pep-6) had no effect on PTHrP-stimulated cAMP formation. Pen-6-cdp itself had no effects on cAMP formation without PTHrP treatment (data not shown). To evaluate PTHR-mediated Gαq/PLC signaling, intracellular calcium mobilization ($[Ca^{2+}]_i$), an index of PLC activity, was measured. Pretreatment with Pen-6-cdp for 2 h concentration-dependently inhibited PTHrP-induced $[Ca^{2+}]_i$ (**Figure 3C**). Collectively, these data demonstrate that the disruptor peptide limits the PTH receptor signaling switch by increasing Gαs/cAMP activation while inhibiting Gαq/PLC signaling.

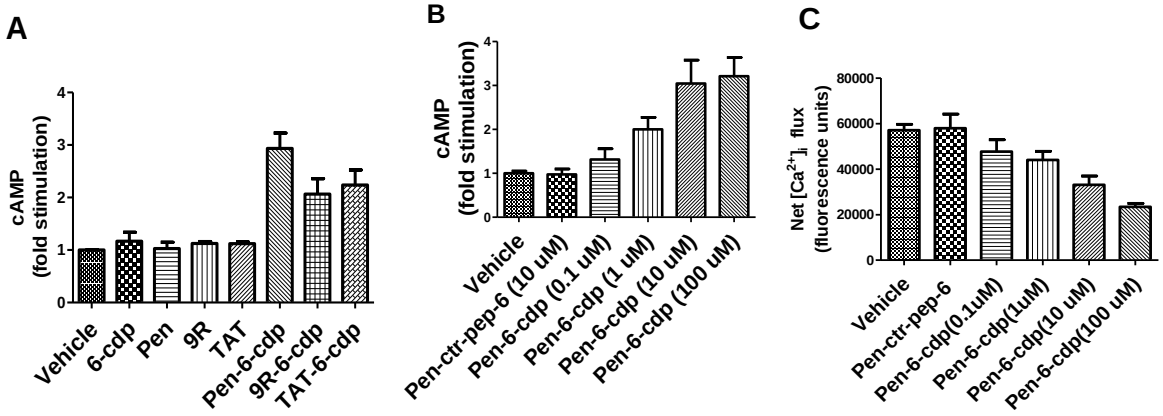

Figure 3. Disruptor peptide (6-cdp) switches PTH receptor signaling from Gαq/PLC to Gαs/cAMP activation. A, Effects of Pen-6-cdp, 9R-6-cdp, TAT-6-cdp, 6-cdp, Pen, 9R or TAT on PTHrP-induced cAMP formation. **B**, Pen-6-cdp increases PTHrP-induced cAMP formation. **C**, Pen-6-cdp inhibits PTHrP-stimulated intracellular calcium.

e. Disruptor peptide has no effect on Wnt3a-induced β-catenin/ T-cell factor (TCF) activation.

ATDC5 cells (chondrogenic cell line) were transfected with TOPflash luciferase reporter plasmid, whose promoter contains a TCF binding region responsive to β-catenin signaling. Cells transfected with the FOPflash reporter plasmid (containing mutated TCF binding region) serve as a control. After 36 h, cells were pretreated with Pen-6-cdp (10 μM) for 2 h, and then Wnt3a (50 ng/ml) was added for 8 h. After treatment, the effect of Pen-6-cdp on Wnt3a-induced β-catenin activation was examined. Our data demonstrated disruptor peptide did not affect the canonical Wnt signaling pathway (**Figure 4**).

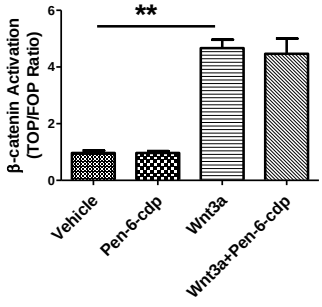

Figure 4. Disruptor peptide does not affect the canonical Wnt pathway. n = 4. **, p<0.01, compared with vehicle control.

f. Disruptor peptide has no cytotoxicity

Different concentrations (1 - 100 µM) of Pen-6-cdp were incubated with ATDC5 cells for 48 h. 3-(4,5-dimethylthiazol-2-yl)-2,5-diphenyltetrazolium bromide (MTT) was then added to each well at a final concentration of 500 µg/ml and incubated for 1 h at 37°C in a 5% CO2 atmosphere. The liquid in the wells was subsequently removed. DMSO was then added to each well, and the absorbance was measured at 570 nm. Data in **Figure 5** showed that Pen-6-cdp did not cause any cytotoxicity in ATDC5 cells.

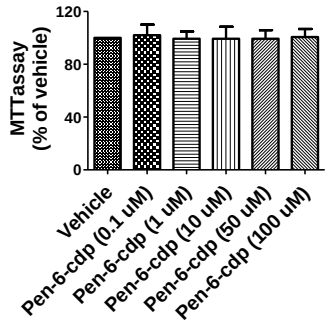

Figure 5. Disruptor peptide does not have cytotoxicity in ATDC5 cells.

g. Disruptor peptide inhibits of the interaction of PTH receptor with β-catenin in ATDC5 cells.

The experiments were performed by immunoprecipitation assay. The ATDC5 cells were treated in the presence or absence of different concentrations of Pen-6-cdp (0.1 – 50 µM). The cells were lysed and solubilized materials were incubated with β-catenin monoclonal antibody for 1 h at 4°C, and then protein G-Sepharose 4B conjugate was added and incubated overnight at 4°C. Total lysates and immunoprecipitated proteins were analyzed by SDS-polyacrylamide gels and the band intensity for β-catenin and PTH receptor was quantified using the Licor Odyssey system. Data in **Figure 6** showed that Pen-6-cdp concentration-dependently inhibited the interaction of PTH receptor interaction with β-catenin.

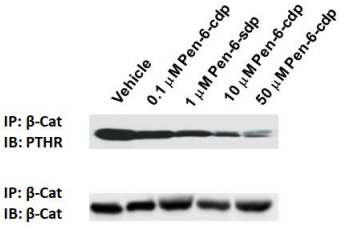

Figure 6. Pen-6-cdp concentration-dependently inhibits the interaction of PTH receptor (PTHR) with β-catenin (β-Cat) in ATDC5 cells. The representative immunoblots are shown. IP: immunoprecipitation; IB: immunoblot.

h. Knockout of β-catenin expression in cells eliminates disruptor peptide effect on PTH receptor signaling.

Endogenous β-catenin expression in mouse ATDC5 cells (chondrogenic cell line) was knocked out using the CRISPR/Cas9 genome-editing technique. **Table 1** lists the single-stranded oligonucleotides encoding a CRISPR targeting RNA (crRNA) of β-catenin that allows sequence-specific targeting of the Cas9 nuclease. The double-stranded oligonucleotides were cloned into linearized GeneArt CRISPR nuclease vectors with an OFP reporter following the manufacturer's protocol (Invitrogen, Carlsbad, CA). Three single colonies were identified for knockout of β-catenin expression in ATDC5 cells by western blotting (**Figure 7**). No β-catenin expression change was observed in cells transfected with control plasmid.

Table 1. CRISPR sequences for knockout of mouse β-catenin

Single stranded Cloning Oligo	Sequences	Accession number
β-catenin	Forward: 5'- CGGGCAGTATGCAATGACTAGTTTT	NM_007614.3
	Reverse: 5'- TAGTCATTGCATACTGCCCGCGGTG	
Control	Forward: 5'- CATTTCTCAGTGCTATAGAGTTTT	
	Reverse: 5'- TCTATAGCACTGAGAAATGCGGTG	

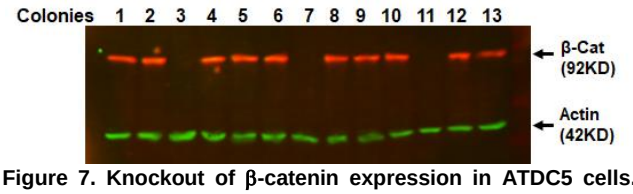

Figure 7. Knockout of β-catenin expression in ATDC5 cells. Actin was used for loading control.

To test whether the specificity of Pen-6-cdp effect on PTHrP-induced cAMP production and intracellular Ca^{2+} mobilization is due to separation of β-catenin from PTHR, we used wild-type (WT Ctr) or β-catenin knockout (β-Cat KO) ATDC5 cells. We demonstrated that Pen-6-cdp failed to enhance PTHrP-induced cAMP formation (**Figure 8A**) and reduce intracellular Ca^{2+} mobilization (**Figure 8B**) in β-catenin knockout cells compared to wild-type ATDC5 cells.

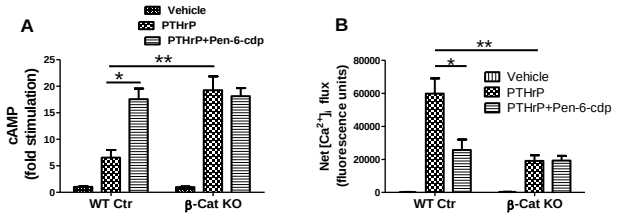

Figure 8. Disruptor peptide fails to affect PTH-induced PTH receptor signaling in β-catenin knockout cells. *, $p< 0.05$, **, $p< 0.01$, compared with WT Ctr cells treated with PTH.

i. Effect of disruptor peptide on inhibition of ATDC5 cell differentiation *in vitro*.

Mouse ATDC5 cells undergo an orderly series of chondrogenic differentiation. After ATDC5 cell confluence, we used chondrogenic medium containing ITS (10 µg/ml insulin, 10 µg/ml transferrin, and 10 ng/ml sodium selenite) to induce ATDC5 cell differentiation in the presence or absence of PTHrP, and disruptor peptide conjugated with penetratin. Mouse primer sequences are listed in **Table 2**. The mRNA expression of type II collagen a1 (Col2a1) and Col10a1 was measured dynamically by quantitative real-time PCR using QuantiTect SYBER Green PCR Kit (Qiagen) and normalized to β-actin mRNA. Vehicle, PTHrP (10 nM) with or without Pen-6-cdp (10 µM) were added to the cultures for the first 6 h of each 48 h cycle. The culture medium was changed to fresh medium every other day. Our results show that PTHrP significantly increased *Col2a1* mRNA expression (**Figure 9**) and inhibited *Col10a1* mRNA expression (**Figure 10**). These effects of PTHrP were further enhanced by the peptide.

Table 2. Mouse primer sequences for real-time PCR

Gene	Sequence	Accession number
Col2a1	Forward: 5'- agg cag aca gta cct tga ga Reverse: 5'- ttg gga tca atc cag tag tc	NM_001113515
Col10a1	Forward: 5'- ctc aaa tac cct ttc tgc tg Reverse: 5'- cct ctt act gga atc cct tt	NM_009925
β-actin	Forward: 5'- aac acc cca gcc atg tac gta g Reverse: 5'- gaa ccg ctc att gcc gat agt	AF122902.1

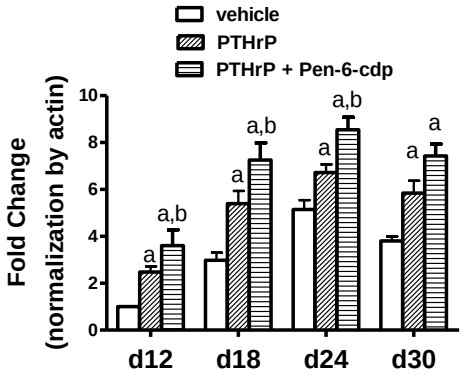

Figure 9. Disruptor peptide enhances PTHrP-induced Col2a1 mRNA expressions in ATDC5 cells. n =4. a, $p<0.05$, compared with vehicle control; b, $p<0.05$, compared with PTHrP.

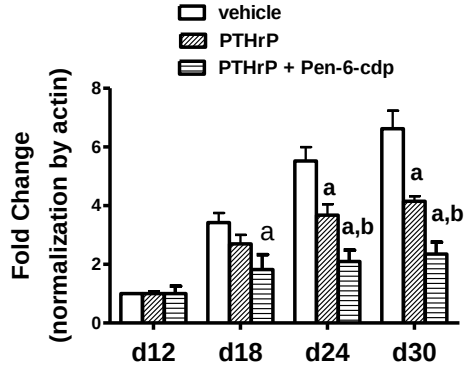

Figure 10. Disruptor peptide promotes PTHrP-inhibition of Col10a1 mRNA expressions in ATDC5 cells. n = 4. a, $p<0.05$, compared with vehicle control; b, $p<0.05$, compared with PTHrP.

j. Effect of disruptor peptide on PTHrP stimulation of cartilage nodule formation.

Chondrocytes derived from 11.5 days of embryo (E11.5) limb bud cells in high density micromass cultures produce extracellular matrix that contains proteoglycans and is positive to Alcian blue staining. The morphology of cartilage nodule formation was visualized dynamically for up to 6 days using EVOS FL Auto Cell Imaging System. The cartilage nodules appeared by day 2 and increased gradually over a 6-day time period (**Figure 11A**). To quantify the Alcian blue staining intensity, the wells in the stained culture plate were extracted with 6 M guanidine HCl for 10 h at

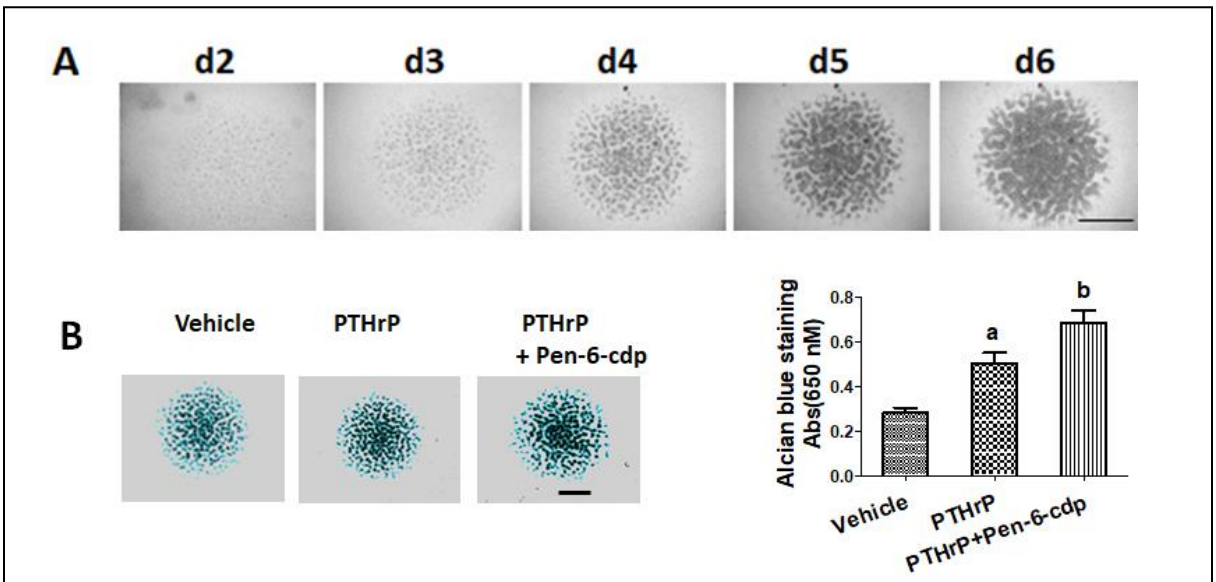

Figure 11. Pen-6-cdp enhances PTHrP-stimulated cartilage nodule formation. **A**. Cartilage nodule formation for d2 to d6. **B**. Effects of PTHrP in the presence or absence of Pen-6-cdp for 4d on cartilage nodule formation. Bar: 2 mm. n = 4. a, $p<0.01$, compared with vehicle control; b, $p<0.05$, compared with PTHrP.

room temperature. The absorbance of the extracted dye was measured at 620 nm. Limb bud mesenchymal cells in micromass cultures express PTH receptor. We assessed the effect of disruptor peptide on cartilage nodule formation induced by PTHrP. PTHrP (10 nM) was added to the culture for the first 6 h of each 48 h cycle for 4 days in the presence or absence of Pen-6cdp (10 μM). The culture medium was changed to fresh medium every other day. Our results show that PTHrP significantly increased cartilage nodule formation compared with vehicle. The disruptor peptide promoted PTHrP stimulation of cartilage nodule formation (**Figure 11B**).

k. Effect of disruptor peptide on PTHrP inhibition of chondrocyte hypertrophy.

Chondrocytes derived from limb bud mesenchymal cells secrete abundant matrix. The cartilaginous tissue was manually removed for histologic evaluation. The expression of Col X level, a chondrocyte hypertrophic marker, was not detected by immunostaining on day 7, but increased on day 21 (**Figure 12**). Treatment with PTHrP in the presence or absence of Pen-6-cdp was the same as

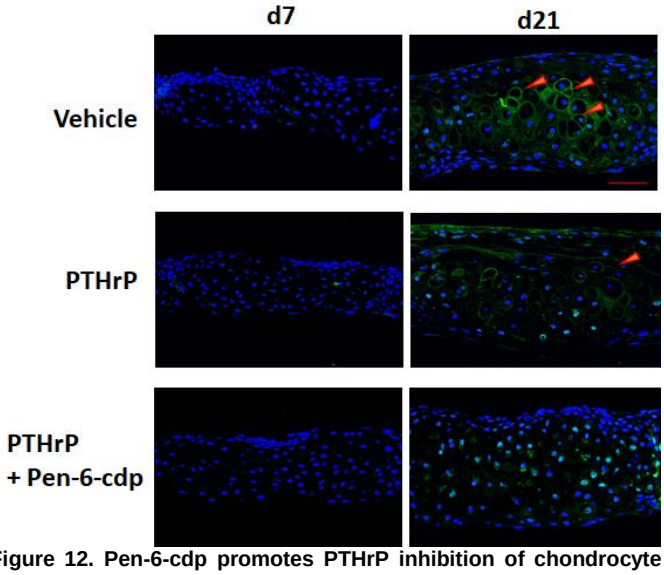

Figure 12. Pen-6-cdp promotes PTHrP inhibition of chondrocyte hypertrophy by reducing Col X expression.

before. PTHrP inhibited Col X expression. Consistent with the effect of the disruptor peptide on cartilage nodule formation, Pen-6-cdp promoted PTHrP inhibition of chondrocyte hypertrophy.

I. Effect of disruptor peptide on inhibition of chondrocyte hypertrophy in muse OA model.

The mouse OA model surgically induced by destabilization of the medial meniscus (DMM) has been commonly used and shares many features of human OA. Mouse DMM model was induced by transection of the meniscotibial ligament in right leg. After 8 weeks, we isolated right and left knee joints. Histological changes and analyses of disease severity were examined by Safranin O staining and Fast green staining, suggesting cartilage damages occurs in the DMM mouse model (**Figure 13**). We then investigated whether disruptor peptide inhibited chondrocyte hypertrophy in this mouse OA model. PTHrP is normally secreted by chondrocytes in low levels and is increased in OA. After mouse DMM surgeries in right legs, we intra-articularly injected Pen-6-cdp (10 µl, 0.1 mM) or vehicle into right knee at the same days. The treatments were 3 times per week for 8 weeks. After termination of treatments, mouse right knee joints were collected, fixed, decalcified, and embedded in paraffin. The expression of chondrocyte hypertrophic marker, Col X and catabolic enzyme [matrix metalloproteinase 13 (MMP13)] was examinated by immunohistochemical assays with Anti-collagen X antibody (Abcam, Cambridge, MA) and MMP13 antibody (Proteintech, Chicago, IL) using detection with 3, 3'-diaminobenzidine (DAB). Data in **Figure 14** showed that the disruptor peptide treatment significantly inhibited both Col X and MMP13 expression in the mouse DMM model.

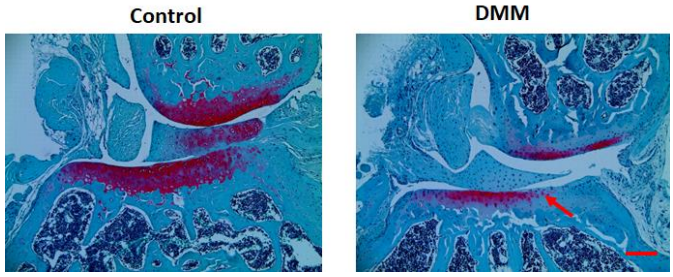

Figure 13. Histological change at 8 weeks following the surgery of destabilization of the medial meniscus (DMM). Slide were stained with Safranin-O and Fast green. Arrow indicates cartilage loss. Scale bar: 100 µm.

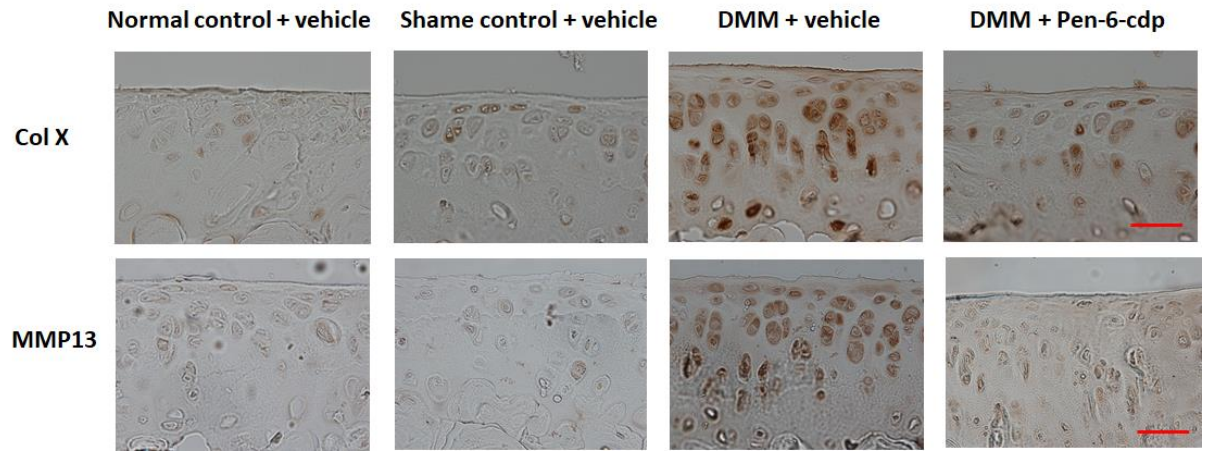

Figure 14. Disruptor peptide inhibits chondrocyte hypertrophy in mouse DMM model by reducing the expression of Col X and MMP13. The representative immunostaining of Col X (top) and MMP13 (bottom) was shown. Scale bar: 100 µm.

3.4. Other achievements

None

What opportunities for training and professional development has the project provided?

Nothing to Report

How were the results disseminated to communities of interest?

Nothing to Report

What do you plan to do during the next reporting period to accomplish the goals?

Nothing to Report

4. IMPACT:

What was the impact on the development of the principal discipline(s) of the project?

We designed a disruptor peptide and have demonstrated that the disruptor peptide blocks the protein interaction of PTH receptor with beta-catenin and inhibits the chondrocyte hypertrophy in relevant cellular and in vivo osteoarthritis models. Our project provides the foundation for further studies of efficacy of the disruptor peptide in different osteoarthritis animal models and human subject testing. Thus, this project provides a rationale and incentive for drug development efforts that the disruptor peptide favors the therapeutic signaling arm and improves the ability of PTHrP to treat/prevent osteoarthritis.

What was the impact on other disciplines?

Nothing to Report

What was the impact on technology transfer?

Nothing to Report

What was the impact on society beyond science and technology?

Nothing to Report

5. CHANGES/PROBLEMS:

Nothing to Report

6. PRODUCTS:

Publications, conference papers, and presentations

Two papers below were supported by this Discovery Award.

(1) Yang Y, Lei H, Qiang YW, **Wang B**. Ixazomib enhances parathyroid hormone (PTH)-induced beta-catenin/T-cell factor (TCF) signaling by dissociating beta-catenin from the PTH receptor. Mol Biol Cell, 2017, 28:1792-1803 PMCID: PMC5491187

(2) Yang Y, Lei H, **Wang B**. Effect of the PTHrP(1-34) analog abaloparatide on inducing chondrogenesis involves inhibition of intracellular reactive oxygen species production. Biochem Biophys Res Commun, 2019, 509: 960-965 PMID: 30654932

Website(s) or other Internet site(s)

Nothing to Report

Technologies or techniques

Nothing to Report

Inventions, patent applications, and/or licenses

Nothing to Report

Other Products

Nothing to Report

7. PARTICIPANTS & OTHER COLLABORATING ORGANIZATIONS

What individuals have worked on the project?

Bin Wang, Ph.D., Principal Investigator (4.8 calendar months), Assistant Professor of Medicine, Center for Translational Medicine, Department of Medicine. As PI, Dr. Wang is responsible for all experiments outlined in the specific aims of the project including the design, performance, analysis, interpretation of experimental studies, preparation of manuscripts, and reporting results of the work.

Irving M Shapiro, BDS, PhD, Other Significant Contributor (no effort requested). Dr. Shapiro is an internationally-recognized cartilage biologist and Anthony and Gertrude DePalma Professor of Orthopaedic Surgery, Director, Division of Orthopaedic Research, Department of Orthopaedic Surgery. He discusses with Dr. Wang about data interpretation, and any design/troubleshooting issues.

Research Technician, Yanmei Yang (12 calendar months), is responsible for routine cell culture, preparing media and buffers for general experiment usage. She performs biochemical experiments, including the cAMP assay, Western blotting and real time PCR, and assist in all other experiments performed by Dr. Wang, including animal studies.

Has there been a change in the active other support of the PD/PI(s) or senior/key personnel since the last reporting period?

Nothing to Report

What other organizations were involved as partners?

Nothing to Report

8. SPECIAL REPORTING REQUIREMENTS

Nothing to Report

9. APPENDICES:

Two papers supported by this Discovery Award are attached.

Ixazomib enhances parathyroid hormone–induced β-catenin/T-cell factor signaling by dissociating β-catenin from the parathyroid hormone receptor

Yanmei Yang[a], Hong Lei[a,b], Ya-wei Qiang[c], and Bin Wang[a,*]
[a]Center for Translational Medicine, Department of Medicine, Sidney Kimmel Medical College, Thomas Jefferson University, Philadelphia, PA 19107; [b]College of Food Science and Engineering, Nanjing University of Finance and Economics, Nanjing 210023, China; [c]Myeloma Institute, University of Arkansas for Medical Sciences, Little Rock, AR 72205

ABSTRACT **The anabolic action of PTH in bone is mostly mediated by cAMP/PKA and Wnt-independent activation of β-catenin/T-cell factor (TCF) signaling. β-Catenin switches the PTH receptor (PTHR) signaling from cAMP/PKA to PLC/PKC activation by binding to the PTHR. Ixazomib (Izb) was recently approved as the first orally administered proteasome inhibitor for the treatment of multiple myeloma; it acts in part by inhibition of pathological bone destruction. Proteasome inhibitors were reported to stabilize β-catenin by the ubiquitin-proteasome pathway. However, how Izb affects PTHR activation to regulate β-catenin/TCF signaling is poorly understood. In the present study, using CRISPR/Cas9 genome-editing technology, we show that Izb reverses β-catenin–mediated PTHR signaling switch and enhances PTH-induced cAMP generation and cAMP response element–luciferase activity in osteoblasts. Izb increases active forms of β-catenin and promotes β-catenin translocation, thereby dissociating β-catenin from the PTHR at the plasma membrane. Furthermore, Izb facilitates PTH-stimulated GSK3β phosphorylation and β-catenin phosphorylation. Thus Izb enhances PTH stimulation of β-catenin/TCF signaling via cAMP-dependent activation, and this effect is due to its separating β-catenin from the PTHR. These findings provide evidence that Izb may be used to improve the therapeutic efficacy of PTH for the treatment of osteoporosis and other resorptive bone diseases.**

Monitoring Editor
Jonathan Chernoff
Fox Chase Cancer Center

Received: Feb 7, 2017
Revised: May 2, 2017
Accepted: May 3, 2017

INTRODUCTION

Long after Bauer and colleagues discovered the anabolic effect of parathyroid hormone (PTH) in 1929 (Bauer *et al.*, 1929), recombinant PTH(1-34) (teriparatide) was approved as the first anabolic agent for the treatment of osteoporosis in the United States in 2002, and no other anabolic drugs are on the market. The optimal use of PTH therapy in osteoporosis depends in part on our understanding of the regulation of PTH signaling to maintain the anabolic actions of PTH while mitigating its catabolic effects. PTH action in bone is mediated by type 1 PTH receptor (PTHR), a member of the G protein–coupled receptor superfamily. Stimulation of PTHR by PTH on osteoblasts leads to activation of Gαs and Gαq, with consequent induction of cAMP/protein kinase A (PKA) and phospholipase C (PLC)/PKC signaling pathways, which results in both osteoblast formation and osteoclast resorption (Qin *et al.*, 2004; Cheloha *et al.*, 2015). Whereas anabolic PTH effects in bone are mediated mostly through the cAMP/PKA signaling pathway, PLC/PKC signaling has been shown to be inhibitory to the osteoanabolic actions of PTH (Ogata *et al.*, 2011). Wnt/β-catenin signaling controls bone formation and homeostasis by increasing osteoblast differentiation and inhibiting osteoclastogenesis (Gaur *et al.*, 2005; Glass *et al.*, 2005;

This article was published online ahead of print in MBoC in Press (http://www.molbiolcell.org/cgi/doi/10.1091/mbc.E17-02-0096) on May 11, 2017.

*Address correspondence to: Bin Wang (bin.wang@jefferson.edu).

Abbreviations used: CREB, cAMP response element–binding protein; CRE-luc, cAMP response element-luciferase; GSK3β, glycogen synthase kinase 3β; GST, glutathione-*S*-transferase; Izb, ixazomib; PKA, protein kinase A; PLC, phospholipase C; PTH, parathyroid hormone; PTHR, PTH receptor; TCF, T-cell factor.

© 2017 Yang *et al.* This article is distributed by The American Society for Cell Biology under license from the author(s). Two months after publication it is available to the public under an Attribution–Noncommercial–Share Alike 3.0 Unported Creative Commons License (http://creativecommons.org/licenses/by-nc-sa/3.0).
"ASCB®," "The American Society for Cell Biology®," and "Molecular Biology of the Cell®" are registered trademarks of The American Society for Cell Biology.

Supplemental Material can be found at:
http://www.molbiolcell.org/content/suppl/2017/05/08/mbc.E17-02-0096v1.DC1

Liu *et al.*, 2015). Our data and those from other groups show that β-catenin interacts with the PTHR and switches the PTHR signaling from Gαs/cAMP to Gαq/PLC activation (Yano *et al.*, 2013; Yang and Wang, 2015). There is cross-talk between PTHR and frizzled receptor to regulate PTH action in bone (Wan *et al.*, 2008; Romero *et al.*, 2010; Revollo *et al.*, 2015). The low-density lipoprotein receptor–related protein 6 (LRP6), one of frizzled's coreceptors, is a key element of the PTH signaling for regulating osteoblast activity (Wan *et al.*, 2008; Revollo *et al.*, 2015). PTHR directly interacts with Dishevelled to regulate β-catenin signaling and osteoclast differentiation (Romero *et al.*, 2010). PTH facilitates canonical Wnt signaling via inactivation of glycogen synthase kinase 3β (GSK3β) in osteoblasts to inhibit β-catenin sequestration (Suzuki *et al.*, 2008). These findings highlight the role of β-catenin/T-cell factor (TCF) signaling in anabolic action of PTH in bone. It is unclear how β-catenin directly contributes to the osteoanabolic action of PTH.

β-Catenin is a multifunctional protein and does not contain a transmembrane domain (Nelson and Nusse, 2004; Stepniak *et al.*, 2009; Marie *et al.*, 2014). Cadherins, which have a single-pass transmembrane domain, bind to β-catenin through their carboxyl-terminal domain at the cytoplasmic tail. Thus β-catenin serves as a link between cadherins and the actin cytoskeleton to mediate the role of cadherins in cell adhesion (Nelson and Nusse, 2004; Stepniak *et al.*, 2009; Marie *et al.*, 2014). In addition, β-catenin also binds to numerous other proteins in a cadherin-independent manner (Bienz and Clevers, 2003; Yano *et al.*, 2013; Yang and Wang, 2015). In bone, N-cadherin associates with β-catenin at the cell membrane to regulate osteoblastogenesis by limiting Wnt signaling. Revollo *et al.* (2015) reported that N-cadherin modulated LRP6-PTHR interaction, restrained the intensity of PTH-induced β-catenin signaling, and reduced bone formation in response to intermittent PTH administration. Moreover, N-cadherin restrains PTH's repressive effects on sclerostin/SOST by regulating LRP6-PTHR interaction (Yang *et al.*, 2016). The interaction of N-cadherin with β-catenin causes increased cadherin abundance on the cell surface and results in β-catenin sequestration at the plasma membrane (Stepniak *et al.*, 2009; Marie *et al.*, 2014). The outcome reduces β-catenin nuclear translocation and decreases TCF/lymphoid enhancer factor–dependent transcriptional activity. Accordingly, blockade of β-catenin degradation may enhance PTH stimulation of β-catenin/TCF signaling.

The ubiquitin-proteasome pathway plays an important role in regulating and controlling bone metabolism (Murray *et al.*, 1998; Garrett *et al.*, 2003; Yang *et al.*, 2015). The first-generation proteasome inhibitor bortezomib has been used as an effective therapy for the treatment of multiple myeloma, a disease characterized by an increase in the activity of osteoclasts and a decrease in the function of osteoblasts adjacent to tumor cells in the bone marrow (Pennisi *et al.*, 2009). Carfilzomib, a next-generation selective proteasome inhibitor, exhibits potent antimyeloma efficacy compared with bortezomib (Herndon *et al.*, 2013; Berenson *et al.*, 2014). We previous reported that carfilzomib suppressed PTH stimulation of osteoclast differentiation and bone-resorptive activity to mitigate the catabolic effects of PTH (Yang *et al.*, 2015). A significant limitation of treatment with bortezomib and carfilzomib is that both drugs are administered intravenously or subcutaneously, which is inconvenient for patients and increases treatment cost. Ixazomib (Izb) is a small-molecule proteasome inhibitor that overcomes these limitations. In November 2015, Izb became the first orally administered proteasome inhibitor approved in the United States as an effective therapy for multiple myeloma. This effect is mediated in part through inhibition of pathologic bone destruction (Kupperman *et al.*, 2010; Garcia-Gomez *et al.*, 2014; Muz *et al.*, 2016). Proteasome inhibitors such as bortezomib and carfilzomib directly stabilize β-catenin protein and increase free cytosolic β-catenin and β-catenin nuclear translocation (Qiang *et al.*, 2009; Hu *et al.*, 2013). However, how proteasome inhibition regulates the complex interplay between PTHR and β-catenin to in turn regulate β-catenin/TCF signaling has not been elucidated.

In the present study, we show that Izb reverses the β-catenin–mediated PTHR signaling switch by enhancing PTH-induced cAMP formation and cAMP response element-luciferase (CRE-luc) reporter gene activity and reducing PTH-stimulated intracellular calcium mobilization in osteoblasts. Izb enhances PTH-induced β-catenin/TCF signaling by separating β-catenin from the PTHR and promoting β-catenin translocation.

RESULTS

Knockout of β-catenin increases PTH-induced cAMP formation and reduces intracellular calcium in osteoblasts

Recent findings show that β-catenin switches the PTHR signaling by binding to the intracellular carboxyl-terminal region of the PTHR in both chondrocytes and HEK293 cells (Yano *et al.*, 2013; Yang and Wang, 2015). In an initial set of experiments, we examined whether β-catenin also switched the PTHR signaling in osteoblasts. Saos2 osteoblastic cells endogenously express both β-catenin and the PTHR (Wang *et al.*, 2009). These cells were transfected with a clustered regularly interspaced short palindromic repeats (CRISPR) construct or CRISPR control plasmid. After 48 h of transfection, the cells were transferred into a 96-well plate with one cell per well by a serial dilution. Two single colonies were identified for knockout of β-catenin expression in Saos2 cells (hereafter referred to as Saos2-β-Cat-KO-3 and Saos2-β-Cat-KO-10 cells; Figure 1A), whereas no β-catenin expression was reduced in cells transfected with control plasmid (Saos2-β-Cat-Ctr; Supplemental Figure S1).

To assess the effect of β-catenin on PTH-induced Gαs/cAMP signaling, we conducted PTH stimulation of cAMP generation in Saos2-β-Cat-KO-3 cells (β-Cat KO) and their control cells (Saos2-β-Cat-Ctr-1, WT Ctr). Knockout of β-catenin significantly increased PTH(1-34) (hereafter referred to as PTH) stimulation of cAMP formation (Figure 1B). To evaluate PTHR-mediated Gαq/PLC signaling, we measured intracellular calcium mobilization ($[Ca^{2+}]_i$), an index of PLC activity, in Saos2-β-Cat-KO-3 cells and Saos2-β-Cat-Ctr-1 cells loaded with the calcium-sensitive dye Fluo-4 AM. Knockout of β-catenin markedly inhibited PTH-induced $[Ca^{2+}]_i$ (Figure 1C). Similar results also occurred in Saos2-β-Cat-KO-10 and Saos2-β-Cat-Ctr-2 cells (unpublished data). Collectively these data clearly demonstrate that knockout of β-catenin reverses the PTHR signaling switch to increase Gαs/cAMP signaling and reduce Gαq/PLC activation, which favors the anabolic PTH action in bone.

Izb enhances PTH-induced cAMP formation in a time- and concentration-dependent manner

We previously reported that proteasome inhibitors stabilized β-catenin by the ubiquitin-proteasome pathway (Qiang *et al.*, 2009; Hu *et al.*, 2013). Because β-catenin switches PTHR signaling, we next determined whether Izb regulated PTHR activation. Izb alone was not able to stimulate cAMP formation (Supplemental Figure S2). However, pretreatment of Izb enhanced PTH stimulation of cAMP formation in Saos2 cells, which exhibited time and concentration dependence. Maximal stimulation by Izb was achieved at 3 h (Figure 2A), but prolonged Izb treatment tended to reduce its effect on PTH-induced cAMP formation. At the 3 h, Izb elicited a concentration-dependent increase in PTH-induced cAMP formation over the range 12.5–100 nM (Figure 2B), but higher concentrations of Izb also decreased its effect on PTH stimulation of cAMP production.

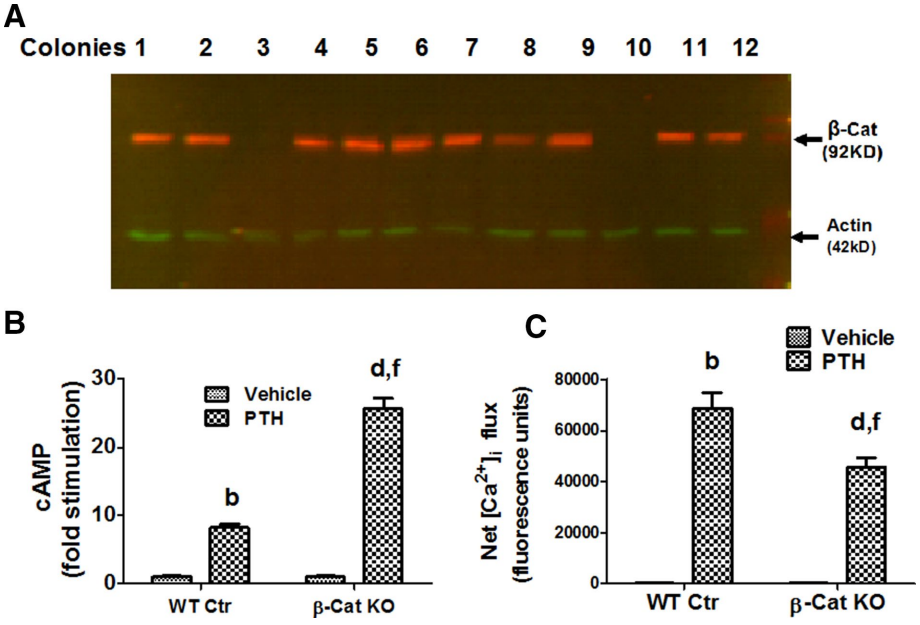

FIGURE 1: Knockout of β-catenin switches the PTHR signaling from Gαq/PLC to Gαs/cAMP activation. Saos2 cells in a six-well plate were transfected with CRISPR construct or control plasmid. After 48 h, the cells, which expressed only OFP reporter as visualized using an Evos machine, were transferred into a 96-well plate with one cell per well. (A) After ~3 wk, two single colonies (Saos2-β-Cat-KO-3 and Saos2-β-Cat-KO-10 cells) were identified for knockout of β-catenin expression in Saos2 cells by Western blotting. Immunoblotting was performed with primary antibodies of mouse monoclonal β-catenin (β-Cat) antibody plus rabbit polyclonal actin antibody and then with secondary antibodies (goat anti-mouse antibody [red] plus goat anti-rabbit antibody [green]). Actin was used for loading control. (B, C) Saos2-β-Cat-KO-3 cells (β-Cat KO) and control Saos2-β-Cat-Ctr-1 cells (WT Ctr) were set up in a 24- or 96-well plate. After 24 h of culture, cells were serum starved overnight. PTH (100 nM) stimulation of intracellular cAMP accumulation (B) or PTH (1 μM) induction of intracellular calcium (C) was measured as described in *Materials and Methods*. Data are summarized as mean ± SE of triplicate measurements. $n = 4$. $^{a}p < 0.05$, $^{b}p < 0.01$, compared with WT Ctr cells treated with vehicle; $^{c}p < 0.05$, $^{d}p < 0.01$, compared with WT Ctr cells treated with PTH; $^{e}p < 0.05$, $^{f}p < 0.01$, compared with β-Cat KO cells treated with vehicle.

Similar to other proteasome inhibitors (Qiang *et al.*, 2009; Hu *et al.*, 2013), Izb but not PTH caused slight cytotoxicity when the cells were treated with it for a prolonged time or at higher concentrations (Supplemental Figure S3, A–C). To reduce the cytotoxicity of Izb, we pretreated Saos2 cells with Izb or vehicle for the first 3 h, followed by an additional 5 h of culture in Izb-free medium, which mimics the pulse treatment used in the clinic and avoids unselective cytotoxicity of proteasome inhibition (Boissy *et al.*, 2008). As expected, this regimen of Izb not only enhanced PTH stimulation of cAMP formation, but it also reduced its cytotoxicity (Figure 2, C and D). To verify these results, we also found that Izb enhanced PTH-induced cAMP generation in mouse primary osteoblasts (Supplemental Figure S4).

Izb promotes PTH stimulation of cAMP formation by facilitating the dissociation of β-catenin from the PTHR

There are different cellular pools of β-catenin in the plasma membrane, cytosol, and nucleus. In most cells, the majority of β-catenin is located at the plasma membrane in a complex with cadherins or other proteins (Stepniak *et al.*, 2009; Marie *et al.*, 2014). Previous findings reported that both bortezomib and carfilzomib increased free and active forms of β-catenin in Saos2 cells (Qiang *et al.*, 2009; Hu *et al.*, 2013). We used an affinity-based E-cadherin–glutathione-*S*-transferase (GST) pull-down assay to separate the free β-catenin from the pool of membrane-bound β-catenin. Saos2 cells were treated with Izb, carfilzomib, or vehicle for the first 3 h, followed by an additional 5 h of culture in Izb- or carfilzomib-free medium. Izb and carfilzomib exhibited increases in the free cytosolic β-catenin level in a concentration-dependent manner (Figure 3A). In addition, Izb increased nuclear β-catenin expression (Figure 3B). An independent experiment performed by confocal microscopy showed that Izb induced β-catenin translocation in Saos2 cells, as shown by its accumulation in cytosol and nucleus (Supplemental Figure S5).

The PTHR is a seven-transmembrane domain protein, whereas β-catenin does not contain any transmembrane domain in its structure. Because Izb increases active forms of β-catenin and promotes β-catenin translocation, we asked whether Izb was able to separate β-catenin from the PTHR at the plasma membrane. Saos2 cells were transfected with pCDNA3.1 vector, hemagglutinin (HA)-PTHR, and/or Flag–β-catenin as indicated. After 48 h of transfection, the cells were treated with vehicle or Izb (100 nM) for 3 h, followed by an additional 5 h of culture in Izb-free medium. The membrane proteins were isolated, and the interaction of Flag-β-catenin with HA-PTHR was performed by immunoprecipitation assay. The result in Figure 3C show that treatment with Izb reduced the interaction of β-catenin with the PTHR at the plasma membrane, further confirming that Izb promotes β-catenin translocation to cytosol and nucleus. As a complementary experiment, Saos2 cells were transiently transfected with green fluorescent protein (GFP)–PTHR. After 48 h of transfection, the cells were treated with vehicle or Izb as before. There was a colocalization of β-catenin with the PTHR at the plasma membrane in the absence of Izb, whereas Izb reduced this colocalization (Figure 3D). Collectively Izb enhanced PTH-induced cAMP generation due to the separation of β-catenin from the PTHR.

Izb regulation of the PTHR signaling is β-catenin dependent

To test whether the specificity of Izb effect on PTH-induced cAMP production is due to separation of β-catenin from the PTHR, we used both wild-type and β-catenin–knockout Saos2 cells. Indeed, Izb failed to enhance PTH-induced cAMP formation and reduce intracellular calcium mobilization in β-catenin–knockout cells compared with that of wild-type Saos2 control cells (Figure 4).

Izb promotes PTH-induced CRE-luc activity and cAMP response element–binding phosphorylation

We next determined the effect of Izb on cAMP/PKA downstream signaling in osteoblasts. The active catalytic subunit of PKA stimulates CRE-luc activity (Castellone *et al.*, 2005). Wild-type Saos2 control cells or Saos2-β-Cat-KO cells were infected with lentiviral particles containing CRE-luc reporter gene. The cells were pretreated with Izb (100 nM for 1 h) before PTH (100 nM) was added to the culture for another 2 h. The CRE-luc activity was then measured. As shown in Figure 5A, Izb itself was not able to stimulate CRE-luc activity in wild-type control or β-catenin–knockout cells. However,

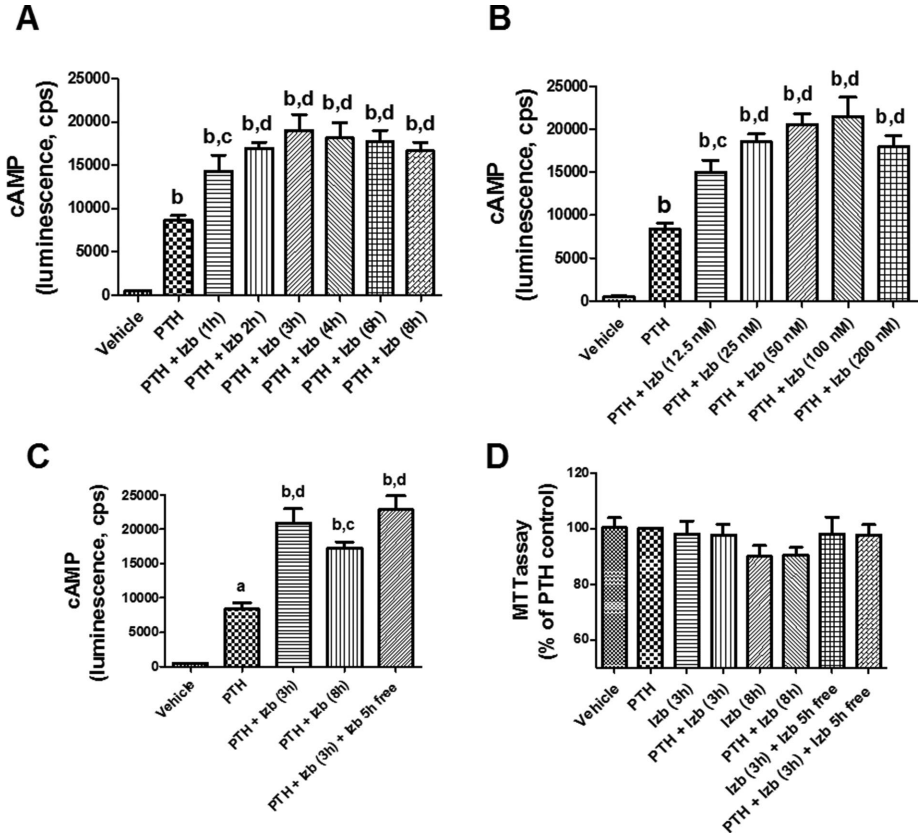

FIGURE 2: Izb enhances PTH-induced cAMP formation in a time- and concentration-dependent manner. (A) Time course of Izb on PTH-stimulated cAMP formation. Saos2 cells were seeded onto a six-well plate. After 90% confluence, the cells were transfected with Glosensor cAMP reporter plasmid (pGS-22F) using Lipofectamine 2000. At 36 h after transfection, cells were transferred into a 96-well plate and cultured for 14 h. The cells were serum starved overnight and then treated with vehicle or Izb (100 nM) for the indicated times, and PTH-induced cAMP formation was measured. The peak response time for cAMP formation is 14 min. (B) Concentration response of Izb on PTH-stimulated cAMP formation. At 3 h, Izb (12.5–100 nM) concentration dependently increased PTH stimulation of cAMP formation. (C) Pulse treatment of Izb increases of PTH-stimulated cAMP formation. Saos2 cells were treated with Izb (100 nM) for 8 h or for the first 3 h followed by an additional 5 h of culture in Izb-free medium in Saos2 cells. (D) Pulse treatment of Izb reduces cytotoxicity. Saos2 cells were treated with Izb (100 nM) for 8 h or for the first 3 h followed by an additional 5 h of culture in Izb-free medium in the presence of PTH (100 nM) in Saos2 cells. Cytotoxicity was assessed by MTT assay as described in *Materials and Methods*. Data are summarized as mean ± SE of triplicate measurements. $n = 3$. $^{a}p < 0.05$, $^{b}p < 0.01$, compared with cells treated with vehicle; $^{c}p < 0.05$, $^{d}p < 0.01$, compared with cells treated with PTH.

knockout of β-catenin significantly increased PTH-induced CRE-luc activity. Izb failed to enhance PTH stimulation of CRE-luc activity in β-catenin–knockout cells compared with wild-type control cells.

cAMP response element–binding (CREB) protein signaling plays a key role in regulating osteoblast activity and bone formation (Long *et al.*, 2001). PTH can induce phosphorylation of CREB through the cAMP/PKA signaling pathway (Pearman *et al.*, 1996; Revollo *et al.*, 2015). Saos2 wild-type cells were pretreated with Izb (100 nM for 2 h) before PTH (100 nM) was added to the culture for another 1 h. PTH markedly induced CREB phosphorylation (Figure 5B). Izb by itself had no effect on phosphorylation of CREB but facilitated PTH stimulation of CREB phosphorylation. Total CREB abundance was unaffected in each group. PKA inhibitor H89 or PKC inhibitor bisindolylmaleimide I (Bis I) alone had no effect on CREB phosphorylation (Supplemental Figure S6). However, H89 but not Bis I blocked Izb enhancement of PTH-induced CREB phosphorylation (Figure 5B). In addition, PTH significantly stimulated CREB phosphorylation in β-catenin–knockout cells, and this change was not affected by Izb in these cells (Figure 5C), further confirming that effects of Izb on PTHR downstream events are β-catenin dependent and mediated by the cAMP/PKA signaling pathway.

Izb enhances PTH stimulation of GSK3β phosphorylation at Ser-9 and β-catenin phosphorylation at Ser-675

The stability of β-catenin is regulated by a multiprotein complex, which includes adenomatous polyposis coli, GSK3β, and axin. PKA phosphorylates GSK3β at the amino acid Ser-9, which inhibits its kinase activity and then inactivates the β-catenin destruction complex (Castellone *et al.*, 2005; Suzuki *et al.*, 2008). PTH induces β-catenin/TCF signaling via inactivation of GSK3β in osteoblasts (Suzuki *et al.*, 2008). Saos2 cells were pretreated with Izb (100 nM) for 2.5 h, and PTH (100 nM) was then added for another 30 min. GSK3β functions upstream of β-catenin activation. As expected, Izb by itself has no effect on GSK3β phosphorylation at Ser-9 (Figure 6A). PTH treatment increased GSK3β phosphorylation, and Izb further enhanced PTH stimulation of GSK3β phosphorylation.

PKA-phosphorylated β-catenin at Ser-675 increases β-catenin accumulation in the cytosol, thereby promoting β-catenin downstream signaling (Taurin *et al.*, 2006; Revollo *et al.*, 2015). We hypothesized that Izb enhanced PTH-induced phosphorylated β-catenin at this site. To test this idea, we pretreated Saos2 cells with Izb for 1 h. Then we added 100 nM PTH to culture for another 2 h. The data in Figure 6B show that PTH stimulated β-catenin phosphorylation at Ser-675. Izb but not PTH slightly increased total β-catenin abundance. However, Izb and PTH synergistically increased β-catenin (Ser-675) phosphorylation, although Izb on its own had no notable effect on the phosphorylation of β-catenin.

Izb promotes PTH-induced β-catenin/TCF signaling in osteoblasts

PTH-facilitated β-catenin/TCF signaling is cAMP/PKA dependent (Kulkarni *et al.*, 2005; Suzuki *et al.*, 2008). Our data show that Izb enhanced PTH-induced cAMP formation and promoted PTH stimulation of GSK3β and β-catenin phosphorylation. These findings suggest an additional mechanism by which Izb enhances PTH-induced β-catenin/TCF signaling in osteoblasts. To test this idea, we transfected Saos2 cells with TOPflash or FOPflash plasmid. The cells were treated with Izb for the first 3 h, followed by an additional 5 h culture in Izb-free medium in the presence or absence of PTH for 8 h. After treatment, the TOPflash and FOPflash reporter activities were measured. Both bortezomib and carfilzomib induce osteoblast differentiation via Wnt-independent induction of β-catenin translocation and activation of β-catenin/TCF signaling (Qiang *et al.*, 2009; Hu *et al.*, 2013). As we predicted, Izb by itself stimulated nuclear β-catenin expression and β-catenin/TCF signaling (Figure 7, A and B). Izb and PTH

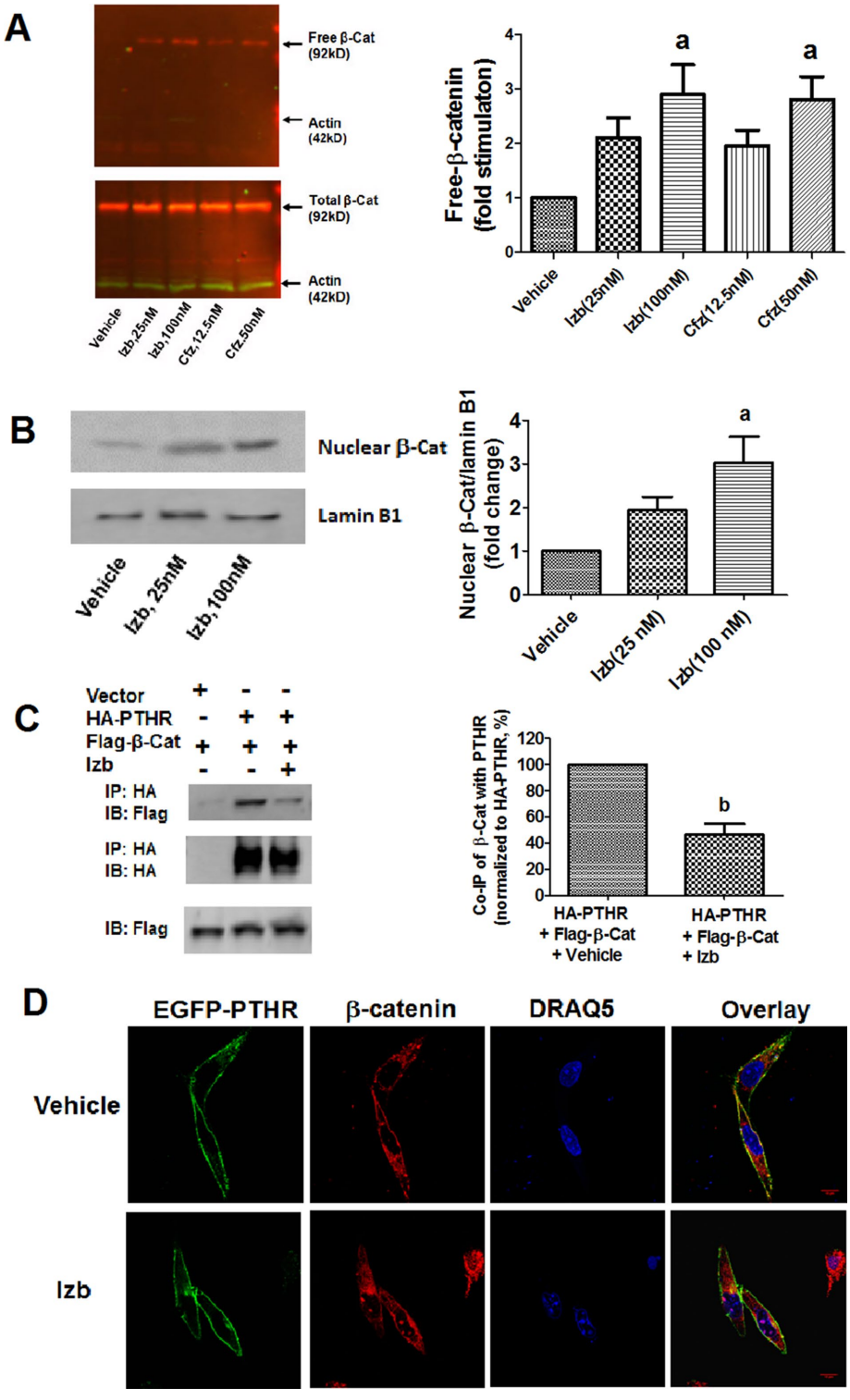

FIGURE 3: Izb facilitates the separation of β-catenin from PTHR. (A) Izb increases free β-catenin protein levels. Left, top, Saos2 cells treated with vehicle, Izb (25, 100 nM), or carfilzomib (Cfz, 12.5, 50 nM) for the first 3 h followed by an additional 5 h of culture in Izb- or Cfz-free medium. GST–E-cadherin was bound to free β-Cat, and the complexes were purified using GST beads. Immunoblotting was then performed with primary antibodies of mouse monoclonal β-Cat antibody plus rabbit polyclonal actin antibody and then with secondary antibodies (goat anti-mouse antibody and goat anti-rabbit antibody). Lack of actin expression suggests that the beads were washed completely. Left, bottom, immunoblotting conducted with total lysates with the same primary antibodies and secondary antibodies. Right, quantified free β-catenin levels in three independent experiments presented as mean ± SE. $^{a}p < 0.05$, $^{b}p < 0.01$, compared with cells treated with vehicle. (B) Izb increases nuclear β-catenin expression. Saos2 cells were treated with vehicle or Izb as in A. Left, nuclear proteins were prepared and β-catenin expression analyzed by immunoblotting. Right, quantified nuclear β-catenin levels in three independent experiments presented as mean ± SE. $^{a}p < 0.05$, $^{b}p < 0.01$, compared with cells treated with vehicle. (C) Saos2 cells were transfected with pCDNA3.1 vector, HA-PTHR, and/or Flag-β-Cat as indicated. After 48 h of transfection, the cells were treated with vehicle or Izb (100 nM) as before. Left, the plasma membrane proteins were isolated, and the interaction of Flag-β-Cat with HA-PTHR measured. Right, coIP of β-catenin with PTHR in three independent experiments normalized to HA-PTHR band. $^{b}p < 0.01$, compared with cells treated with vehicle. (D) Saos2 cells were transfected with GFP-PTHR. After 48 h, the cells were treated with vehicle or Izb (100 nM) as before. The cells were fixed, stained, and visualized for colocalization of PTHR with β-catenin by confocal microscopy. Representative of three independent experiments performed with similar results. Scale bar, 10 μm.

synergistically increased nuclear β-catenin levels and β-catenin/TCF activation. Similar results were also identified in mouse osteoblasts (Supplemental Figure S7). PKA inhibitor H89 but not PKC inhibitor Bis I inhibited PTH-stimulated TCF reporter activity (Figure 7B), confirming that PTH-stimulated β-catenin/TCF signaling is cAMP/PKA dependent. However, H89 only partially reversed the effect of Izb on PTH stimulation of β-catenin/TCF activation. Furthermore, H89 failed to affect Izb increase of free cytosolic β-catenin level, nuclear β-catenin expression (Supplemental Figure S8, A and B), and β-catenin/TCF signaling (Supplemental Figure S8D). H89 also had no effect on β-catenin phosphorylation at Ser-675 in the presence of Izb (Supplemental Figure S8C). These data clearly demonstrate that the effect of Izb alone on β-catenin translocation and β-catenin/TCF signaling is not related to a cAMP/PKA pathway. Together the results show that, in addition to being capable of promoting β-catenin translocation, Izb enhances PTH stimulation of β-catenin/TCF signaling via an increase in cAMP-dependent signaling.

DISCUSSION

Although PTHR signaling pathways are being studied in increasing detail, the regulation of PTHR functions has not been fully elucidated. The anabolic PTH effects on bone are mostly mediated by the Gαs/cAMP signaling pathway, whereas Gαq/PLC activation may antagonize these osteoanabolic actions (Datta and Abou-Samra, 2009;

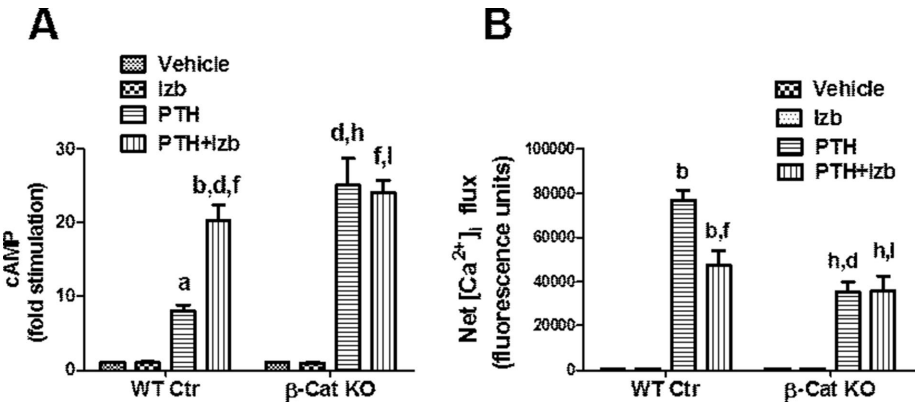

FIGURE 4: Izb blocks β-catenin–mediated PTHR signaling switch. Saos2-β-Cat-KO-3 cells (β-Cat KO) and their control cells (Saos2-β-Cat-Ctr-1, WT Ctr) were seeded onto a 24- or 96-well plate. After confluence, the cells were serum starved overnight and then pretreated with Izb (100 nM) for 3 h. PTH stimulation of cAMP formation (A) and intracellular calcium (B) were measured. Data are summarized as mean ± SE of triplicate measurements. $n = 3$. [a]$p < 0.05$, [b]$p < 0.01$, compared with WT Ctr cells treated with vehicle; [c]$p < 0.05$, [d]$p < 0.01$, compared with WT Ctr cells treated with PTH; [e]$p < 0.05$, [f]$p < 0.01$, compared with WT Ctr cells treated with Izb; [g]$p < 0.05$, [h]$p < 0.01$, compared with β-Cat KO cells treated with vehicle; [i]$p < 0.05$, [j]$p < 0.01$, compared with β-Cat KO cells treated with PTH; [k]$p < 0.05$, [l]$p < 0.01$, compared with β-Cat KO cells treated with Izb.

Ogata *et al.*, 2011). Additional anabolic signaling by PTH action involves the canonical β-catenin pathway, which is independent of Wnt. Therefore manipulating PTHR signaling by shifting Gαq/PLC to Gαs/cAMP activation and increasing β-catenin/TCF signaling represents a means of maintaining the anabolic actions of PTH.

Sequences located at the carboxyl terminus of PTHR control its signaling (Datta and Abou-Samra, 2009; Romero *et al.*, 2011). PTHR has a PSD-95/Discs large/ZO-1 (PDZ) motif located in the last four amino acids, which interact with NHERF1 and NHERF2 (Romero *et al.*, 2011; Vilardaga *et al.*, 2011). As originally described by Mahon *et al.* (2002), NHERF2, a NHERF1 homologue, markedly inhibits adenylyl cyclase by stimulating inhibitory Gαi proteins in PS120 cells transfected with the PTHR. In contrast, no differences of PTH-stimulated cAMP formation were noted between wild-type and NHERF1-null proximal tubule cells (Cunningham *et al.*, 2005) in the presence or absence of NHERF1. In ROS17/2.8 cells or primary osteoblasts, NHERF1 increases PTH-stimulated cAMP accumulation (Wheeler *et al.*, 2008; Wang *et al.*, 2013). Moreover, truncation of the carboxyl-terminal region of the PTHR that lacks determinants for stable β-arrestin association (PTHR-480stop) enhances PTH stimulation of adenylyl cyclase but not PLC (Iida-Klein *et al.*, 1995; Wang *et al.*, 2007). In contrast to the aforementioned regulatory proteins, β-catenin specifically binds to the intracellular carboxyl-terminal region of the PTHR and switches the PTHR signaling from Gαs/cAMP to Gαq/PLC activation in chondrocytes and HEK293 cells (Yano *et al.*, 2013; Yang and Wang, 2015). As an initial step, we determined whether this signaling switch by β-catenin also occurred in osteoblasts. To that end, we generated a β-catenin–knockout cell line in osteoblasts using CRISPR/Cas9 genome-editing technology. Our data showed that knockout of β-catenin (i.e., zero expression of β-catenin) significantly increased PTH-induced cAMP formation, whereas PTH-stimulated PLC activity was markedly reduced in these knockout cells compared with cells transfected with CRISPR/Cas9 control plasmid (Figure 1). These data are consistent with a previous study, using small interfering RNA, demonstrating that knockdown of β-catenin (i.e., reduction of β-catenin expression) inhibited the PTHR signaling switch (Yano *et al.*, 2013). These findings raised an important question of whether the intervention of β-catenin interaction with PTHR in osteoblasts has a similar effect to alter PTH-induced PTHR signaling. Proteasome inhibitors such as bortezomib and carfilzomib, which have been used to treat multiple myeloma patients, were shown to directly stabilize β-catenin protein and increase β-catenin nuclear translocation (Qiang *et al.*, 2009; Hu *et al.*, 2013). In the present study, we chose Izb, the first orally administered proteasome inhibitor for the treatment of multiple myeloma, because it has the potential to treat resorptive bone diseases such as osteoporosis. We found that Izb increased active β-catenin expression and translocation (Figure 3 and Supplemental Figure S5). Most importantly, we found, using coimmunoprecipitation (coIP) and confocal microscopy, that Izb was able to separate β-catenin from the PTHR at the cell membrane. Pretreatment of Izb increased PTH-stimulated cAMP production and reduced PTH-induced PLC activity (Figure 4 and Supplemental Figure S4), demonstrating that Izb can inhibit the PTHR signaling switch to increase cAMP formation in osteoblasts by promoting the dissociation of β-catenin from the PTHR. To the best of our knowledge, this is the first report showing how a proteasome inhibitor regulates PTHR signaling by dissociating β-catenin from the PTHR.

It is established that PTH-induced β-catenin/TCF signaling is cAMP/PKA dependent (Kulkarni *et al.*, 2005; Suzuki *et al.*, 2008). CRE-luc activity and CREB phosphorylation are downstream events that depend on cAMP/PKA activation. We demonstrated that Izb by itself had no effect on CRE-luc activity and CREB phosphorylation but enhanced PTH stimulation of CRE-luc activity and phosphorylation of CREB (Figure 5). Furthermore, Izb and PTH synergistically increased GSK3β phosphorylation at Ser-9 and phosphorylated β-catenin at Ser-675 (Figure 6), the outcome of which results in β-catenin translocation to the nucleus. It is known that PTH-induced β-catenin/TCF activation takes >6 h. Similar to other proteasome inhibitors, Izb treatment in cells for >3 h has some cytotoxicity (Boissy *et al.*, 2008). To maintain Izb biological activity and avoid its toxicity, Saos2 cells received Izb for the first 3 h, followed by an additional 5 h of culture in Izb-free medium. Our findings show that Izb enhanced PTH-induced β-catenin/TCF signaling without inducing cytotoxicity (Figures 2 and 7). Therefore our work reveals a novel role for Izb in regulating PTH-induced β-catenin/TCF signaling via the cAMP/PKA-dependent pathway.

The increase of cytosolic and nuclear β-catenin by proteasome inhibition is via its specific inhibition of β-catenin degradation but independent of Wnt ligands and not related to GSK3β phosphorylation (Qiang *et al.*, 2009). In the present study, we demonstrated that Izb by itself does not affect GSK3β phosphorylation at Ser-9 and β-catenin phosphorylation at Ser-675. Thus the underlying mechanisms by which Izb induces β-catenin/TCF signaling are not fully understood. Proteasome inhibition can stabilize numerous proteins. PTHR directly interacts with Dishevelled to regulate β-catenin signaling (Romero *et al.*, 2010). Zhou *et al.* (2016) recently reported that ubiquitin-specific protease 4 strongly inhibited Wnt/β-catenin signaling by removing lysine-63 linked polyubiquitin chain from Dishevelled and antagonized osteoblast differentiation

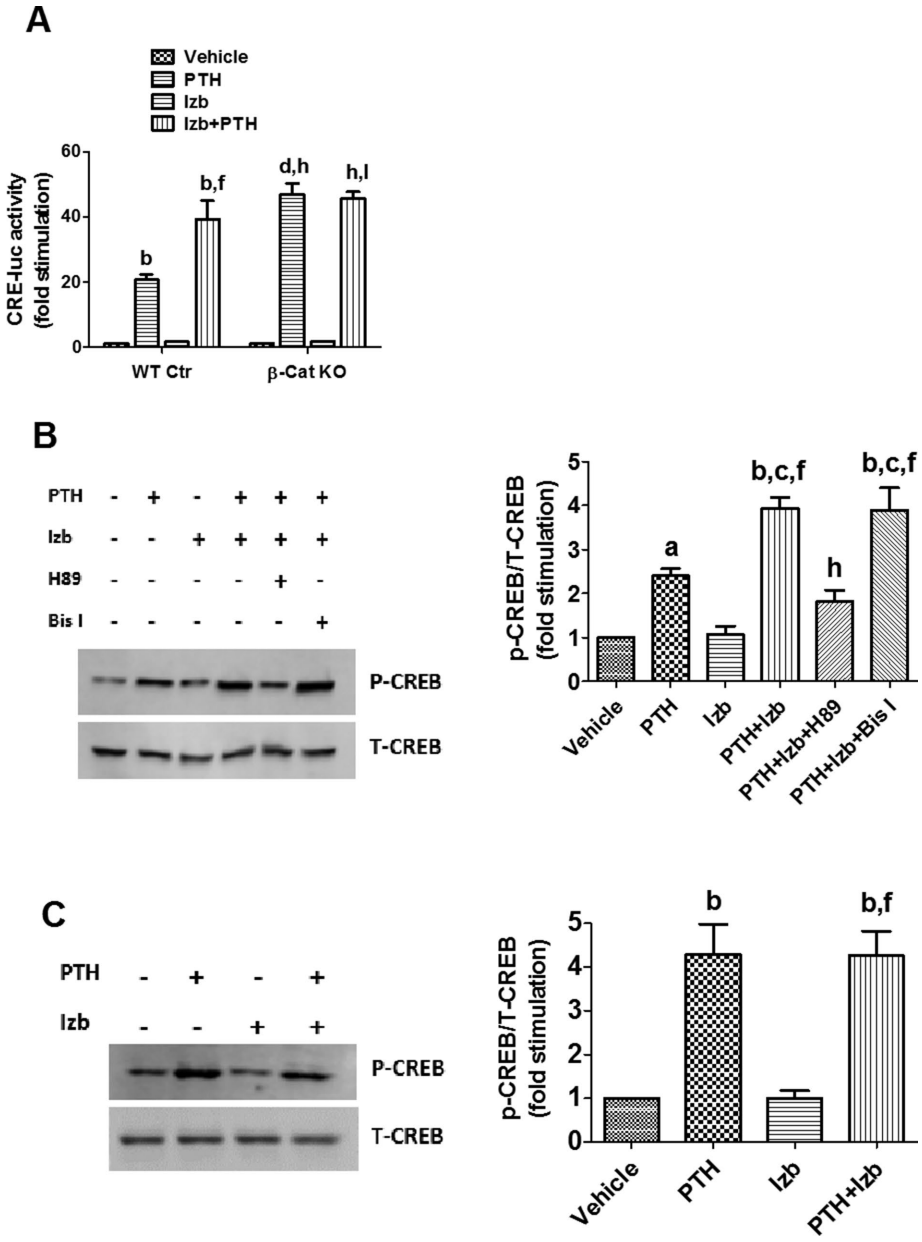

FIGURE 5: Izb enhances PTH-induced CRE-luc activity and CREB phosphorylation. (A) Knockout of β-catenin increases PTH-induced CRE-luc activity. Saos2-β-Cat-KO-3 cells (β-Cat KO) and their control cells (Saos2-β-Cat-Ctr-1, WT Ctr) were seeded onto a 24-well plate. After cells reached 80% confluence, the cells were infected with lentiviral particles of CRE-luc reporter and cultured for 48 h. The cells were serum starved overnight and then pretreated with Izb (100 nM for 1 h) before PTH (100 nM) was added to the culture for another 2 h. PTH induction of CRE-luc activity in each group was measured as described in *Material and Methods*. Data are summarized as mean ± SE of triplicate measurements. $n = 3$. $^{a}p < 0.05$, $^{b}p < 0.01$, compared with WT Ctr cells treated with vehicle; $^{c}p < 0.05$, $^{d}p < 0.01$, compared with WT Ctr cells treated with PTH; $^{e}p < 0.05$, $^{f}p < 0.01$, compared with WT Ctr cells treated with Izb; $^{g}p < 0.05$, $^{h}p < 0.01$, compared with β-Cat KO cells treated with vehicle; $^{i}p < 0.05$, $^{j}p < 0.01$, compared with β-Cat KO cells treated with PTH; $^{k}p < 0.05$, $^{l}p < 0.01$, compared with β-Cat KO cells treated with Izb. (B) Izb enhancement of PTH-induced CREB phosphorylation is cAMP/PKA dependent. Saos2-β-Cat-Ctr-1 cells (WT Ctr) were pretreated with Izb (100 nM for 2 h) before PTH (100 nM) was added to the culture for another 1 h in the presence or absence of PKA inhibitor H89 (10 μM) or PKC inhibitor Bis I (10 μM) for 1 h and 15 min. Left, PTH-induced CREB phosphorylation and total CREB expression (loading control). Right, quantified CREB phosphorylation and total CREB expression in four independent experiments presented as mean ± SE. $^{a}p < 0.05$, $^{b}p < 0.01$, compared with cells treated with vehicle; $^{c}p < 0.05$, $^{d}p < 0.01$, compared with cells treated with PTH; $^{e}p < 0.05$, $^{f}p < 0.01$, compared with cells treated with Izb; $^{g}p < 0.05$, $^{h}p < 0.01$, compared with cells treated with PTH plus Izb. (C) Izb fails to affect PTH stimulation of CREB phosphorylation in β-catenin–knockout cells. Saos2-β-Cat-KO-3 cells (β-Cat KO) cells were pretreated with Izb (100 nM for 2 h) before PTH (100 nM) was added to the culture for another 1 h. Left, PTH stimulation of CREB phosphorylation. Right, quantified CREB phosphorylation and total CREB expression in three independent experiments presented as mean ± SE. $^{a}p < 0.05$, $^{b}p < 0.01$, compared with cells treated with vehicle; $^{c}p < 0.05$, $^{d}p < 0.01$, compared with cells treated with PTH; $^{e}p < 0.05$, $^{f}p < 0.01$, compared with cells treated with Izb.

and mineralization through Dishevelled degradation. Therefore we do not exclude the possibility that Izb enhancement of PTH stimulation of β-catenin/TCF signaling may be related to its inhibition of Dishevelled degradation. In addition, PTHR activation, desensitization, endocytosis, and recycling proceed in a cyclical manner. We previously reported that PTHR recycling was complete by 2 h after stimulation with PTH(1-34), a biologically active peptide fragment, suggesting the PTHR trafficking is different from that of β-catenin. However, PTH(7-34), which does not activate the PTHR but promotes receptor internalization, down-regulates the PTHR by a ubiquitin-sensitive pathway (Sneddon *et al.*, 2003; Alonso *et al.*, 2011). Continuous and high-dose PTH(1-34) causes bone resorption and hypercalcemia (Qin *et al.*, 2004; Cheloha *et al.*, 2015). Future investigations will need to assess the roles of proteasome inhibition on prolonged PTH treatment in induction of both cAMP formation and β-catenin/TCF signaling in bone cells.

On the basis of the present findings and generally accepted roles of proteasome inhibitor and β-catenin/TCF, we propose a model (Figure 8) for the effect of Izb on regulation of PTHR signaling cascade in bone. According to this notion, Izb regulates PTHR signaling by dissociating β-catenin from the PTHR to enhance PTH-induced β-catenin/TCF activity. Such an effect is cAMP/PKA dependent. Izb has been applied for the treatment of both the tumor burden and bone loss associated with multiple myeloma. Whereas our previous study emphasized that proteasome inhibition mitigated the catabolic effect of PTH on bone by suppressing PTH-induced osteoclast differentiation and bone-resorptive activity (Yang *et al.*, 2015), the present study demonstrates that Izb can regulate the PTHR signaling in osteoblasts, which favors anabolic PTH action in bone. These findings warrant further investigation of this combination of PTH and Izb on osteoblast differentiation

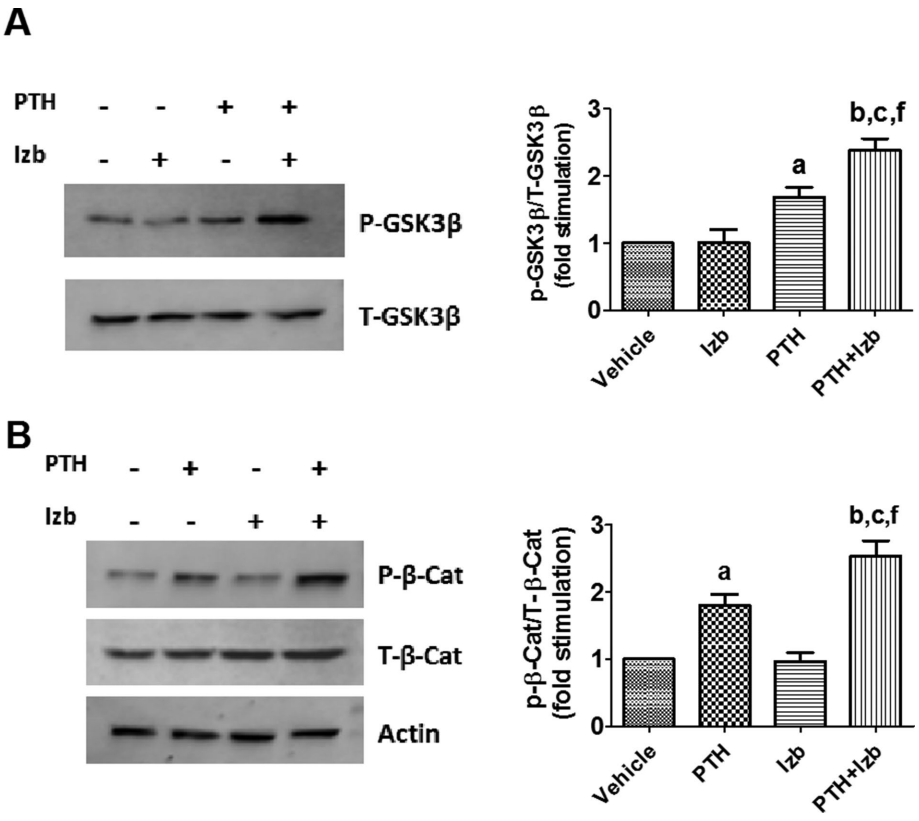

FIGURE 6: Izb facilitates PTH stimulation of GSK3β and β-catenin phosphorylation. (A) Saos2 cells were seeded onto a six-well plate. After confluence, the cells were serum starved overnight and then pretreated with Izb (100 nM) for 2.5 h, and PTH (100 nM) was then added to the culture for another 30 min. Left, PTH-induced GSK3β phosphorylation and total GSK3β expression. Right, quantified GSK3β phosphorylation at Ser-9 and total GSK3β expression in four independent experiments presented as mean ± SE. (B) Saos2 cells were grown in a six-well plate and cultured as before. The cells were pretreated with Izb (100 nM) for 1 h, and PTH (100 nM) was then added to the culture for another 2 h. Left, PTH-induced β-catenin phosphorylation at Ser-675 and total β-catenin expression. Actin was used for loading control. Right, quantified β-catenin phosphorylation and total β-catenin expression in four independent experiments presented as mean ± SE. $^{a}p < 0.05$, $^{b}p < 0.01$, compared with cells treated with vehicle; $^{c}p < 0.05$, $^{d}p < 0.01$, compared with cells treated with PTH; $^{e}p < 0.05$, $^{f}p < 0.01$, compared with cells treated with Izb.

and osteogenesis in vitro and therapeutic efficacy in animal models of osteoporosis.

MATERIALS AND METHODS

Human [Nor^{8,18},Tyr^{34}]PTH(1-34) was purchased from Bachem California (Torrance, CA). Carfilzomib was purchased from LC Laboratories (Woburn, MA), and Izb was obtained from Selleck Chemicals (Houston, TX). Both drugs were prepared in a 10 mM stock solution in dimethyl sulfoxide (DMSO) and diluted in plain medium just before use. Antibodies of β-catenin phosphorylation at Ser-675, phospho-GSK3β (Ser-9), GSK3β, phospho-CREB, and CREB were obtained from Cell Signaling Technology (Danvers, MA). HA.11 ascites monoclonal antibody (mAb) and HA.11 monoclonal affinity matrix were purchased from Covance (Berkeley, CA). Actin polyclonal antibody and lamin B1 mAb were from Santa Cruz Biotechnology (Santa Cruz, CA). Mouse monoclonal β-catenin antibody and Fluo-4 AM were obtained from BD Biosciences (San Jose, CA). Lentiviral particles of reporter gene CRE-luc were from Qiagen (Germantown, MD). GeneArt CRISPR Nuclease Vector with orange fluorescent protein (OFP) reporter kit (A21174), α-MEM, Opti-MEM, and Lipofectamine 2000 were purchased from Invitrogen (Carlsbad, CA). Glosensor cAMP reporter plasmid (pGS-22F) was purchased from Promega (Madison, WI). Protease inhibitor cocktail Set I, H89, and Bis I were from Calbiochem (San Diego, CA). The Cyclic AMP Direct EIA Kit was purchased from Arbor Assays (Ann Arbor, MI). Ionomycin was from EMD Millipore (Billerica, MA). All other reagents were from Sigma-Aldrich (St. Louis, MO).

Cell culture

Saos2 cells, a human osteoblast–like cell line, were purchased from the American Type Culture Collection (ATCC; Manassas, VA) and cultured in DMEM/F-12 with 10% fetal bovine serum (FBS), 100 U/ml penicillin, and 100 μg/ml streptomycin. MC4 osteoblastic cells (subclone 4 of MCT3-E1; ATCC) were cultured in α-MEM with 10% FBS in the presence of 50 μg/ml ascorbic acid for 5 d and then used in the experiments. All cells were maintained at 37°C in a humidified atmosphere of 5% CO_2 and 95% air.

Primary osteoblast culture

All of the experiments using mice for generation of primary osteoblasts were performed according to the protocol approved by the Animal Care and Use Committee of Thomas Jefferson University. Generation of primary osteoblast cultures was described previously (Yang *et al.*, 2015). Briefly, calvariae were removed from 2- to 3-d-old C57BL/6 mice and digested with 1 mg/ml collagenase type II and 0.25% trypsin-EDTA. Cells released from the second and third digestions were grown in α-MEM supplemented with 10% FBS, 100 U/ml penicillin, and 100 μg/ml streptomycin. After trypsinization of the confluent cells, differentiating osteoblasts were cultured in the presence of 50 μg/ml ascorbic acid for 7 d and used in the experiments.

cAMP formation and detection

Saos2 cells were transfected with Glosensor cAMP reporter plasmid (pGS-22F) in a six-well plate by Lipofectamine 2000 following the manufacturer's instruction. After 36 h of transfection, cells were transferred into a 96-well plate. The confluent cells were then treated with vehicle or Izb (100 nM) at the indicated time points. After treatment, cells were incubated with luciferin for 20 min at room temperature, and then PTH or vehicle was added. Luminescence arising from intracellular cAMP binding to the Glosensor reporter protein was measured in real time at 2-min intervals for 60 min using a plate reader (Synergy-2; Gidon *et al.*, 2014; Carter *et al.*, 2015). The peak response time occurred by 16 min.

Additional cAMP measurements were performed in primary osteoblasts and Saos2-β-Cat-KO cells and Saos2-β-Cat-Ctr cells. These cells were treated with vehicle or Izb (100 nM for 3 h). PTH (100 nM for 15 min)-induced cAMP formation was detected using the cyclic AMP Direct EIA Kit (Arbor Assays) following the supplier's instructions. The samples were analyzed by using a cAMP standard curve.

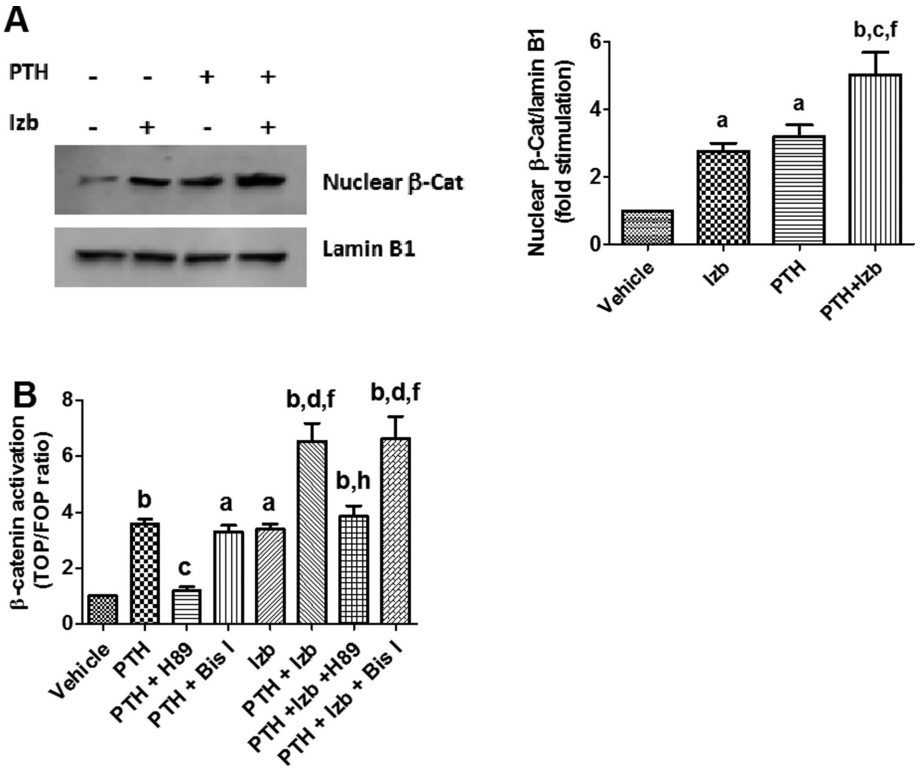

FIGURE 7: Izb facilitates PTH-induced Wnt/β-catenin signaling. (A) Izb enhances PTH-stimulated nuclear β-catenin expression. Saos2 cells were treated with Izb (100 nM) for the first 3 h, followed by an additional 5 h of culture in Izb-free medium in the presence or absence of PTH (100 nM) for 8 h. Left, nuclear proteins were prepared and β-catenin expression was analyzed by immunoblotting. Right, quantified nuclear β-catenin expression in four independent experiments presented as mean ± SE. $^{a}p < 0.05$, $^{b}p < 0.01$, compared with cells treated with vehicle; $^{c}p < 0.05$, $^{d}p < 0.01$, compared with cells treated with PTH; $^{e}p < 0.05$, $^{f}p < 0.01$, compared with cells treated with Izb. (B) Izb promotes PTH-induced TCF reporter activity. Saos2 cells were seeded into a 12-well plate. After 90% confluence, the cells were transfected with TOPflash or FOPflash plasmid. At 36 h after transfection, the cells were serum starved for 12 h and then treated with Izb for the first 3 h, followed by an additional 5 h of culture in Izb-free medium in the presence or absence of PTH (100 nM), PKA inhibitor H89 (5 μM), or PKC inhibitor Bis I (5 μM) for 8 h. The β-catenin/TCF activation was measured as described in *Materials and Methods*. Data are summarized as mean ± SE of triplicate measurements. $n = 3$. $^{a}p < 0.05$, $^{b}p < 0.01$, compared with cells treated with vehicle; $^{c}p < 0.05$, $^{d}p < 0.01$, compared with cells treated with PTH; $^{e}p < 0.05$, $^{f}p < 0.01$, compared with cells treated with PTH plus Izb.

Cell viability assay

Cell viability was measured as described previously (Yang *et al.*, 2015). Briefly, 3-(4,5-dimethylthiazol-2-yl)-2,5-diphenyltetrazolium bromide (MTT) was added to each well at a final concentration of 500 μg/ml. The cells were further incubated for 1 h at 37°C in a 5% CO_2 atmosphere, and the liquid in the wells was subsequently removed. DMSO was then added to each well, and the absorbance was measured at 570 nm.

Knockout of β-catenin gene expression in Saos2 cells

Constitutive β-catenin expression in Saos2 cells was knocked out using the CRISPR/Cas9 genome-editing technique. Table 1 lists the double-stranded oligonucleotides encoding a CRISPR targeting RNA (crRNA) of β-catenin that allows sequence-specific targeting of the Cas9 nuclease. The double-stranded oligonucleotides were cloned into linearized GeneArt CRISPR nuclease vectors with an OFP reporter following the manufacturer's protocol. Saos2 cells were seeded into a six-well plate. After cells reached 90% confluence, CRISPR plasmid or control plasmid was transfected into the cells using Lipofectamine 2000 following the manufacturer's protocol. Two days after the transfection, the cells were counted and seeded into a 96-well plate with one cell per well by a serial dilution. OFP reporter was applied to monitor transfection efficiency in cells for fluorescence-based tracking using an Evos machine (Invitrogen). After ~3 wk, Western blotting was used to screen β-catenin expression in cells. Zero expression of β-catenin was identified in two single colonies when the cells were transfected with CRISPR construct, whereas β-catenin expression was not changed in cells transfected with the control plasmid.

Intracellular calcium assay

Saos2 cells were seeded into poly-D-lysine–coated 96-well plates and grown to confluence. The cells were then treated with vehicle or Izb (100 nM) for 3 h. After treatment, the cells were loaded with 2 μM Fluo-4 AM according to the manufacturer's protocol. PTH or vehicle was added by an automated pipetting system in triplicate, and the 525-nm signals were generated by excitation at 485 nm with a Flex Station II (Molecular Devices, Sunnyvale, CA) as previously reported (Deshpande *et al.*, 2014). Maximal Ca^{2+} response was determined by stimulating the cells with 1 μM ionomycin. The net peak Ca^{2+} response was calculated using the equation (maximum agonist-induced fluorescence units) − (basal fluorescence units).

CRE-luc assay

Saos2 cells were infected with lentiviral particles of CRE reporter. After 48 h, the cells were serum starved overnight and then treated with Izb, PTH, or vehicle at the indicated time points. The CRE-luc activity was detected as previously described (Yan *et al.*, 2011).

Cell fractionation

Membrane and nuclear proteins were prepared by fractionating cell lysates using differential centrifugation at 4°C as described previously (Wang *et al.*, 2008; Hu *et al.*, 2013). Briefly, cells treated with Izb, PTH, or vehicle were harvested in hypotonic buffer (10 mM 4-(2-hydroxyethyl)-1-piperazineethanesulfonic acid, pH 7.4, 1 mM $MgCl_2$, 0.5 mM $CaCl_2$, 1 mM EDTA) supplemented with protease inhibitor cocktail set I and then homogenized by 30 strokes of a Dounce homogenizer. After removal of the nuclear pellet, lysates were separated into cytosolic and membrane fractions by ultracentrifugation (100,000 × *g*) for 60 min. The membrane proteins were used for the interaction of β-catenin with the PTHR, and the nuclear proteins were subjected to immunoblot analysis for β-catenin expression.

Immunoprecipitation and immunoblot analysis

The plasma membrane proteins were solubilized in immunoprecipitation assay buffer (1% Nonidet P-40, 0.5% Na deoxycholate, 0.1% SDS, 50 mM Tris, pH 7.4, and 150 mM NaCl) supplemented with

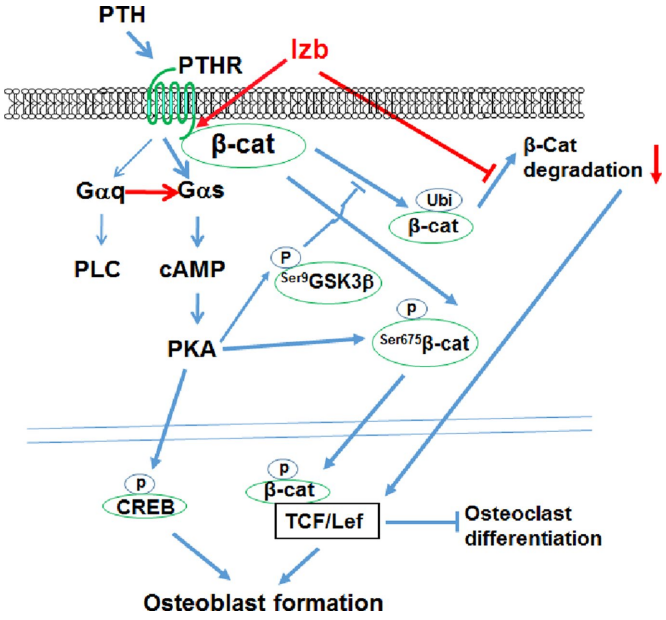

FIGURE 8: Model of Izb regulation of PTHR signaling cascade in bone. Both PTH and Izb are able to induce β-catenin (β-Cat)/TCF signaling. Izb stabilizes β-Cat by inhibiting its proteasome degradation. β-Cat–mediated PTHR signaling switch is blocked by Izb due to its promoting of β-Cat translocation, thereby dissociating β-Cat from the PTHR. Izb facilitates PTH stimulation of CREB phosphorylation, β-Cat (Ser-675) phosphorylation, GSK3β (Ser-9) phosphorylation, and TCF/Lef activity through a cAMP/PKA signaling pathway. Collectively these findings suggest that the combination of PTH and Izb favors the anabolic PTH action in bone.

protease inhibitor cocktail set I. HA beads were added to equal amounts of soluble membrane proteins in each group. Immunoprecipitated proteins, nuclear proteins, or total lysates (Wang *et al.*, 2008; Hu *et al.*, 2013) were analyzed by SDS–polyacrylamide gels and transferred to Immobilon-P membranes (Millipore) using the semidry method (Bio-Rad). Membranes were blocked with 3% bovine serum albumin in Tris-buffered saline/Tween 20 buffer at room temperature for 1 h and incubated with different antibodies overnight at 4°C. The membranes were then washed and incubated with IRDye 800CW goat anti-rabbit immunoglobulin G (IgG) or IRDye 680RD goat anti-mouse IgG at room temperature for 1 h. Band intensity was quantified using the LI-COR Odyssey system (Yang and Wang, 2015).

Double-stranded cloning Oligo	Sequence	Accession number
β-Catenin	Forward: 5′-TCCCACTAATGTCCAGCGTT	NM_001904
	Reverse: 5′-AACGCTGGACATTAGTGGGA	
Control	Forward: 5′-CATTTCTCAGTGCTATAGA	
	Reverse: 5′-TCTATAGCACTGAGAAATG	

TABLE 1: CRISPR sequences for knockout of human β-catenin.

GST–E-cadherin pull-down assay

The GST–E-cadherin binding assay was performed as described (Qiang *et al.*, 2009). The β-catenin–binding site of E-cadherin was cloned as a GST-fusion protein, and complexes were purified using GST beads. GST–E-cadherin was used to precipitate uncomplexed β-catenin from 500 μg of cell lysates. The free β-catenin fraction detected by immunoblotting represents active forms of β-catenin (Qiang *et al.*, 2009).

Fluorescence staining

Saos2 cells were grown on glass coverslips and then transfected with GFP-PTHR. After 40 h, the cells were incubated with vehicle or Izb (100 nM) for 3 h, followed by an additional 5 h of culture in Izb-free medium. The cells were rinsed in phosphate-buffered saline (PBS), fixed on 4% paraformaldehyde for 10 min, and then permeabilized with 0.2% Triton X-100 for 15 min at room temperature. Blocking was performed by incubating the cells for 1 h at room temperature in 10% goat serum in PBS. Anti–β-catenin mouse mAb diluted (1:250) in blocking buffer was applied to the specimens for 1 h at room temperature. Alexa Fluor 546–tagged goat anti-mouse secondary antibody diluted 1:1000 was applied under the same conditions as the primary antibody. Nucleus staining was performed with DRAQ5. Coverslips were mounted for confocal microscopy (Wang *et al.*, 2008).

TOPflash/FOPflash activity assay

Saos2 cells or MC4 cells were transfected with TOPflash or FOPflash in a 12-well plate by using Lipofectamine 2000 according to the manufacturer's protocol. After 36 h of transfection, cells were serum starved for 12 h and then treated with the indicated reagents. Eight hours after treatment, cells were lysed with reporter lysis buffer (Promega). The cell lysates were then drawn four times through a 21-gauge needle attached to a 1-ml syringe. The supernatants were transferred to a 96-well plate. The luminescence of each well was recorded after addition of BioGlo Luciferase substrate (Promega). The ratio of TOP/FOP signal was calculated and normalized to control conditions.

Statistical analysis

The data are presented as mean ± SE of triplicate measurements. In the figures, *n* indicates the number of independent experiments. Statistical analysis between control and treated groups was performed using Student's *t* test. Multiple comparisons in one or two types of cells were evaluated by one-way or two-way analysis of variance followed by Bonferroni's posttest (Prism; GraphPad). $p < 0.05$ was considered sufficient to reject the null hypothesis.

ACKNOWLEDGMENTS

We thank Raymond B. Penn for help in the completion of this work. This work was supported, in whole or in part, by National Institutes of Health Grants AR062705 and AR063289 and Department of Defense Grant PR152096 to B.W.

REFERENCES

Alonso V, Magyar CE, Wang B, Bisello A, Friedman PA (2011). Ubiquitination-deubiquitination balance dictates ligand-stimulated PTHR sorting. J Bone Miner Res 26, 2923–2934.

Bauer W, Aub JC, Albright F (1929). Studies of calcium and phosphorus metabolism: V. A study of the bone trabeculae as a readily available reserve supply of calcium. J Exp Med 49, 145–162.

Berenson JR, Hilger JD, Yellin O, Dichmann R, Patel-Donnelly D, Boccia RV, Bessudo A, Stampleman L, Gravenor D, Eshaghian S, *et al.* (2014).

Replacement of bortezomib with carfilzomib for multiple myeloma patients progressing from bortezomib combination therapy. Leukemia 28, 1529–1536.
Bienz M, Clevers H (2003). Armadillo/beta-catenin signals in the nucleus–proof beyond a reasonable doubt. Nat Cell Biol 5, 179–182.
Boissy P, Andersen TL, Lund T, Kupisiewicz K, Plesner T, Delaisse JM (2008). Pulse treatment with the proteasome inhibitor bortezomib inhibits osteoclast resorptive activity in clinically relevant conditions. Leuk Res 32, 1661–1668.
Carter PH, Dean T, Bhayana B, Khatri A, Rajur R, Gardella TJ (2015). Actions of the small molecule ligands SW106 and AH-3960 on the type-1 parathyroid hormone receptor. Mol Endocrinol 29, 307–321.
Castellone MD, Teramoto H, Williams BO, Druey KM, Gutkind JS (2005). Prostaglandin E2 promotes colon cancer cell growth through a Gs-axin-beta-catenin signaling axis. Science 310, 1504–1510.
Cheloha RW, Gellman SH, Vilardaga JP, Gardella TJ (2015). PTH receptor-1 signalling-mechanistic insights and therapeutic prospects. Nat Rev Endocrinol 11, 712–724.
Cunningham R, E X, Steplock D, Shenolikar S, Weinman EJ (2005). Defective PTH regulation of sodium-dependent phosphate transport in NHERF-1-/- renal proximal tubule cells and wild-type cells adapted to low-phosphate media. Am J Physiol Renal Physiol 289, F933–F938.
Datta NS, Abou-Samra AB (2009). PTH and PTHrP signaling in osteoblasts. Cell Signal 21, 1245–1254.
Deshpande DA, Yan H, Kong KC, Tiegs BC, Morgan SJ, Pera T, Panettieri RA, Eckhart AD, Penn RB (2014). Exploiting functional domains of GRK2/3 to alter the competitive balance of pro- and anticontractile signaling in airway smooth muscle. FASEB J 28, 956–965.
Garcia-Gomez A, Quwaider D, Canavese M, Ocio EM, Tian Z, Blanco JF, Berger AJ, Ortiz-de-Solorzano C, Hernandez-Iglesias T, Martens AC, *et al.* (2014). Preclinical activity of the oral proteasome inhibitor MLN9708 in myeloma bone disease. Clin Cancer Res 20, 1542–1554.
Garrett IR, Chen D, Gutierrez G, Zhao M, Escobedo A, Rossini G, Harris SE, Gallwitz W, Kim KB, Hu S, *et al.* (2003). Selective inhibitors of the osteoblast proteasome stimulate bone formation in vivo and in vitro. J Clin Invest 111, 1771–1782.
Gaur T, Lengner CJ, Hovhannisyan H, Bhat RA, Bodine PV, Komm BS, Javed A, van Wijnen AJ, Stein JL, Stein GS, *et al.* (2005). Canonical WNT signaling promotes osteogenesis by directly stimulating Runx2 gene expression. J Biol Chem 280, 33132–33140.
Gidon A, Al-Bataineh MM, Jean-Alphonse FG, Stevenson HP, Watanabe T, Louet C, Khatri A, Calero G, Pastor-Soler NM, Gardella TJ, *et al.* (2014). Endosomal GPCR signaling turned off by negative feedback actions of PKA and v-ATPase. Nat Chem Biol 10, 707–709.
Glass DA 2nd, Bialek P, Ahn JD, Starbuck M, Patel MS, Clevers H, Taketo MM, Long F, McMahon AP, Lang RA, *et al.* (2005). Canonical Wnt signaling in differentiated osteoblasts controls osteoclast differentiation. Dev Cell 8, 751–764.
Herndon TM, Deisseroth A, Kaminskas E, Kane RC, Koti KM, Rothmann MD, Habtemariam B, Bullock J, Bray JD, Hawes J, *et al.* (2013). U.S. Food and Drug Administration approval: carfilzomib for the treatment of multiple myeloma. Clin Cancer Res 19, 4559–4563.
Hu B, Chen Y, Usmani SZ, Ye S, Qiang W, Papanikolaou X, Heuck CJ, Yaccoby S, Williams BO, Van Rhee F, *et al.* (2013). Characterization of the molecular mechanism of the bone-anabolic activity of carfilzomib in multiple myeloma. PLoS One 8, e74191.
Iida-Klein A, Guo J, Xie LY, Juppner H, Potts JT Jr, Kronenberg HM, Bringhurst FR, Abou-Samra AB, Segre GV (1995). Truncation of the carboxyl-terminal region of the rat parathyroid hormone (PTH)/PTH-related peptide receptor enhances PTH stimulation of adenylyl cyclase but not phospholipase C. J Biol Chem 270, 8458–8465.
Kulkarni NH, Halladay DL, Miles RR, Gilbert LM, Frolik CA, Galvin RJ, Martin TJ, Gillespie MT, Onyia JE (2005). Effects of parathyroid hormone on Wnt signaling pathway in bone. J Cell Biochem 95, 1178–1190.
Kupperman E, Lee EC, Cao Y, Bannerman B, Fitzgerald M, Berger A, Yu J, Yang Y, Hales P, Bruzzese F, *et al.* (2010). Evaluation of the proteasome inhibitor MLN9708 in preclinical models of human cancer. Cancer Res 70, 1970–1980.
Liu B, Wu S, Han L, Zhang C (2015). beta-catenin signaling induces the osteoblastogenic differentiation of human pre-osteoblastic and bone marrow stromal cells mainly through the upregulation of osterix expression. Int J Mol Med 36, 1572–1582.
Long F, Schipani E, Asahara H, Kronenberg H, Montminy M (2001). The CREB family of activators is required for endochondral bone development. Development 128, 541–550.
Mahon MJ, Donowitz M, Yun CC, Segre GV (2002). Na(+)/H(+) exchanger regulatory factor 2 directs parathyroid hormone 1 receptor signalling. Nature 417, 858–861.
Marie PJ, Hay E, Modrowski D, Revollo L, Mbalaviele G, Civitelli R (2014). Cadherin-mediated cell-cell adhesion and signaling in the skeleton. Calcif Tissue Int 94, 46–54.
Murray EJ, Bentley GV, Grisanti MS, Murray SS (1998). The ubiquitin-proteasome system and cellular proliferation and regulation in osteoblastic cells. Exp Cell Res 242, 460–469.
Muz B, Ghazarian RN, Ou M, Luderer MJ, Kusdono HD, Azab AK (2016). Spotlight on ixazomib: potential in the treatment of multiple myeloma. Drug Des Dev Ther 10, 217–226.
Nelson WJ, Nusse R (2004). Convergence of Wnt, beta-catenin, and cadherin pathways. Science 303, 1483–1487.
Ogata N, Shinoda Y, Wettschureck N, Offermanns S, Takeda S, Nakamura K, Segre GV, Chung UI, Kawaguchi H (2011). G{alpha}q signal in osteoblasts is inhibitory to the osteoanabolic action of parathyroid hormone. J Biol Chem 286, 13733–13740.
Pearman AT, Chou WY, Bergman KD, Pulumati MR, Partridge NC (1996). Parathyroid hormone induces c-fos promoter activity in osteoblastic cells through phosphorylated cAMP response element (CRE)-binding protein binding to the major CRE. J Biol Chem 271, 25715–25721.
Pennisi A, Li X, Ling W, Khan S, Zangari M, Yaccoby S (2009). The proteasome inhibitor, bortezomib suppresses primary myeloma and stimulates bone formation in myelomatous and nonmyelomatous bones in vivo. Am J Hematol 84, 6–14.
Qiang YW, Hu B, Chen Y, Zhong Y, Shi B, Barlogie B, Shaughnessy JD Jr (2009). Bortezomib induces osteoblast differentiation via Wnt-independent activation of beta-catenin/TCF signaling. Blood 113, 4319–4330.
Qin L, Raggatt LJ, Partridge NC (2004). Parathyroid hormone: a double-edged sword for bone metabolism. Trends Endocrinol Metab 15, 60–65.
Revollo L, Kading J, Jeong SY, Li J, Salazar V, Mbalaviele G, Civitelli R (2015). N-cadherin restrains PTH activation of Lrp6/beta-catenin signaling and osteoanabolic action. J Bone Miner Res 30, 274–285.
Romero G, Sneddon WB, Yang Y, Wheeler D, Blair HC, Friedman PA (2010). Parathyroid hormone receptor directly interacts with dishevelled to regulate beta-catenin signaling and osteoclastogenesis. J Biol Chem 285, 14756–14763.
Romero G, von Zastrow M, Friedman PA (2011). Role of PDZ proteins in regulating trafficking, signaling, and function of GPCRs: means, motif, and opportunity. Adv Pharmacol 62, 279–314.
Sneddon WB, Syme CA, Bisello A, Magyar CE, Rochdi MD, Parent JL, Weinman EJ, Abou-Samra AB, Friedman PA (2003). Activation-independent parathyroid hormone receptor internalization is regulated by NHERF1 (EBP50). J Biol Chem 278, 43787–43796.
Stepniak E, Radice GL, Vasioukhin V (2009). Adhesive and signaling functions of cadherins and catenins in vertebrate development. Cold Spring Harb Perspect Biol 1, a002949.
Suzuki A, Ozono K, Kubota T, Kondou H, Tachikawa K, Michigami T (2008). PTH/cAMP/PKA signaling facilitates canonical Wnt signaling via inactivation of glycogen synthase kinase-3beta in osteoblastic Saos-2 cells. J Cell Biochem 104, 304–317.
Taurin S, Sandbo N, Qin Y, Browning D, Dulin NO (2006). Phosphorylation of beta-catenin by cyclic AMP-dependent protein kinase. J Biol Chem 281, 9971–9976.
Vilardaga JP, Romero G, Friedman PA, Gardella TJ (2011). Molecular basis of parathyroid hormone receptor signaling and trafficking: a family B GPCR paradigm. Cell Mol Life Sci 68, 1–13.
Wan M, Yang C, Li J, Wu X, Yuan H, Ma H, He X, Nie S, Chang C, Cao X (2008). Parathyroid hormone signaling through low-density lipoprotein-related protein 6. Genes Dev 22, 2968–2979.
Wang B, Bisello A, Yang Y, Romero GG, Friedman PA (2007). NHERF1 regulates parathyroid hormone receptor membrane retention without affecting recycling. J Biol Chem 282, 36214–36222.
Wang B, Yang Y, Abou-Samra AB, Friedman PA (2009). NHERF1 regulates parathyroid hormone receptor desensitization: Interference with beta-arrestin binding. Mol Pharmacol 75, 1189–1197.
Wang B, Yang Y, Friedman PA (2008). Na/H exchange regulatory factor 1, a novel AKT-associating protein, regulates extracellular signal-regulated kinase signaling through a B-Raf-mediated pathway. Mol Biol Cell 19, 1637–1645.
Wang B, Yang Y, Liu L, Blair HC, Friedman PA (2013). NHERF1 regulation of PTH-dependent bimodal Pi transport in osteoblasts. Bone 52, 268–277.

Wheeler D, Garrido JL, Bisello A, Kim YK, Friedman PA, Romero G (2008). Regulation of parathyroid hormone type 1 receptor dynamics, traffic, and signaling by the Na+/H+ exchanger regulatory factor-1 in rat osteosarcoma ROS 17/2.8 cells. Mol Endocrinol 22, 1163–1170.

Yan H, Deshpande DA, Misior AM, Miles MC, Saxena H, Riemer EC, Pascual RM, Panettieri RA, Penn RB (2011). Anti-mitogenic effects of beta-agonists and PGE2 on airway smooth muscle are PKA dependent. FASEB J 25, 389–397.

Yang H, Dong J, Xiong W, Fang Z, Guan H, Li F (2016). N-cadherin restrains PTH repressive effects on sclerostin/SOST by regulating LRP6-PTH1R interaction. Ann NY Acad Sci 1385, 41–52.

Yang Y, Blair HC, Shapiro IM, Wang B (2015). The proteasome inhibitor carfilzomib suppresses parathyroid hormone-induced osteoclastogenesis through a RANKL-mediated signaling pathway. J Biol Chem 290, 16918–16928.

Yang Y, Wang B (2015). Disruption of beta-catenin binding to parathyroid hormone (PTH) receptor inhibits PTH-stimulated ERK1/2 activation. Biochem Biophys Res Commun 464, 27–32.

Yano F, Saito T, Ogata N, Yamazawa T, Iino M, Chung UI, Kawaguchi H (2013). beta-Catenin regulates parathyroid hormone/parathyroid hormone-related protein receptor signals and chondrocyte hypertrophy through binding to the intracellular C-terminal region of the receptor. Arthritis Rheum 65, 429–435.

Zhou F, Li F, Fang P, Dai T, Yang B, van Dam H, Jia J, Zheng M, Zhang L (2016). Ubiquitin-specific protease 4 antagonizes osteoblast differentiation through dishevelled. J Bone Miner Res 31, 1888–1898.

Biochemical and Biophysical Research Communications 509 (2019) 960–965

Contents lists available at ScienceDirect

Biochemical and Biophysical Research Communications

journal homepage: www.elsevier.com/locate/ybbrc

Effect of the PTHrP(1-34) analog abaloparatide on inducing chondrogenesis involves inhibition of intracellular reactive oxygen species production

Yanmei Yang [a], Hong Lei [a, b], Bin Wang [a, *]

[a] Center for Translational Medicine, Department of Medicine, Sidney Kimmel Medical College, Thomas Jefferson University, 1020 Locust Street, Philadelphia, PA, 19107, USA
[b] College of Food Science and Engineering, Nanjing University of Finance and Economics, Nanjing, 210023, China

ARTICLE INFO

Article history:
Received 20 December 2018
Accepted 9 January 2019
Available online 14 January 2019

Keywords:
Abaloparatide
Osteoarthritis
Chondrogenesis
Mesenchymal stem cells
Reactive oxygen species

ABSTRACT

Osteoarthritis (OA) is a degenerative joint disease characterized by a progressive loss of articular cartilage. Mesenchymal stem cells transplanted to damaged tissues are promising for OA cartilage repair. However, these cells are poor survival after transplantation and acquire hypertrophic properties during chondrogenic induction. Parathyroid hormone-related protein (PTHrP) promotes chondrogenesis and suppresses chondrocyte hypertrophic differentiation. Additionally, PTHrP was reported to have antioxidant effects. The synthetic PTHrP(1-34) analog abaloparatide (ABL) is a newly approved drug for osteoporosis therapy. It is unknown whether ABL stimulates chondrogenesis and affects intracellular reactive oxygen species (ROS) production. By using mouse embryonic limb bud mesenchymal stem cells in micromass culture as an *in vitro* model of chondrogenic differentiation, we found that mesenchymal stem cells in micromass cultures spontaneously produced ROS, and N-acetyl-L-cysteine, a potent antioxidant, enhanced chondrogenesis. The effect of ABL on stimulation of chondrogenesis is involved in its inhibition of intracellular ROS generation. These novel findings support the use of ABL for the damaged cartilage regeneration.

© 2019 Elsevier Inc. All rights reserved.

1. Introduction

Osteoarthritis (OA) is a common age-related joint disease characterized by a progressive loss of articular cartilage [1]. Because the root causes of joint degeneration in OA remain unclear, current treatments for OA are palliative to alleviate symptoms in the early stage, while surgical options exist for advanced disease. Human articular cartilage has a poor self-healing capacity once damaged due to its avascular and aneural nature. Currently, cell-based therapies are promising for regeneration of the damaged articular cartilages and restoration of their function [2,3]. Mesenchymal stem cells maintain self-renewal capacity and are capable to differentiate into chondrocytes and other cell types. In spite of several advantages of mesenchymal stem cells, they have not achieved satisfactory effects so far, mostly due to low survival rate following transplantation and the onset of chondrocyte hypertrophy [4,5]. Thus, molecules that facilitate the selective differentiation of mesenchymal stem cells into chondrocytes are potentially capable of repairing the damaged articular cartilage in OA patients.

Parathyroid hormone-related protein (PTHrP) is a heterogeneous polypeptide with amino-terminal sequence homology to PTH. Both PTH and PTHrP bind to the type 1 PT H/PTHrP receptor (PTH1R). Chondrocytes and osteoblasts express PTH1R [6,7]. Signaling through the PTH1R regulates bone remodeling and maintains the articular chondrocyte phenotype under healthy conditions [8,9]. The synthetic PTHrP(1-34) analog abaloparatide (ABL) was approved in the United States in 2017 for osteoporosis therapy in an attempt to improve the anabolic effects of PTH1R signaling [10]. However, the therapeutic effect of ABL on osteoarthritis has not been extensively studied compared with that on osteoporosis.

Recent findings indicate that some characteristics of OA, such as the expression of hypertrophic markers, resemble chondrocyte differentiation processes in endochondral ossification [11,12]. The

* Corresponding author. Center for Translational Medicine, Department of Medicine, Sidney Kimmel Medical College, Thomas Jefferson University, 1020 Locust Street, Philadelphia, PA, 19107, USA
E-mail address: bin.wang@jefferson.edu (B. Wang).

https://doi.org/10.1016/j.bbrc.2019.01.049
0006-291X/© 2019 Elsevier Inc. All rights reserved.

entire process of endochondral ossification includes mesenchymal cell condensation, chondrogenic differentiation, chondrocyte hypertrophy and apoptosis, and matrix calcification. High-density micromass culture is a well-established *in vitro* model that mimics mesenchymal cell condensation to trigger a cascade of chondrogenesis during growth plate development *in vivo* [11,12]. Thus, targeting the onset of mesenchymal stem cell differentiation to chondrocytes may be useful to assess the efficacy of candidate molecules for regeneration of the damaged articular cartilages and restoration of their function. Oxidative stress can cause mesenchymal cell death during isolation and processing of these cells from their natural niche [13]. Both PTH(1-34) and PTHrP(1-36) have anti-oxidant effects [14,15]. In the present study, we have investigated whether mouse mesenchymal stem cells in micromass cultures produce reactive oxygen species (ROS) and effect of ABL on stimulation of chondrogenesis is related to its inhibition of intracellular ROS production.

2. Materials and methods

2.1. Materials

Human $Nle^{8,18}$, Tyr^{34}-PTH(1-34), which is a sulfur-free and biologically active peptide fragment of PTH (hereafter referred to as PTH(1-34), was purchased from Bachem (Torrance, CA). ABL ([$Glu^{22,25}$, $Leu^{23,28,31}$, Aib^{29}, $Lys^{26,30}$] PTHrP [1-34]), in which Aib is α-aminoisobutyric acid, was synthesized by PEPTIDE 2.0 (Chantilly, VA). TRIzol, DNase, and Alexa Fluor 488-tagged goat-anti-rabbit second antibody were from Invitrogen (Carlsbad, CA). AccuScript high fidelity 1st strand cDNA synthesis kit was from Stratagene (La Jolla, CA). iTag™ SYBR Green Supermix with ROX was from Bio-Rad (Hercules, CA). Anti-collagen X antibody and In Situ apoptosis detection kit were purchased from Abcam (Cambridge, MA). All other reagents were from Sigma-Aldrich (St. Louis, MO).

2.2. Isolation and culture of mesenchymal cells and articular chondrocytes

All of the experiments employing mice for generation of primary mesenchymal cells from 11.5-day pregnant female mice and primary chondrocytes from 2-3-day-old C57BL/6 mice were performed according to the protocol approved by the Animal Care and Use Committee of Thomas Jefferson University. Limb bud mesenchymal cells were isolated from 11.5-day pregnant female C57BL/6 mice as previously described [12]. Mice were mated overnight and mating was confirmed by the presence of a vaginal plug (considered as 0.5 days of gestation). On day 11.5 of gestation, pregnant mice were euthanized by CO_2 and followed by cervical dislocation. The uterus was removed and washed in sterile calcium and magnesium-free phosphate-buffered saline in the presence of fungizone (1.25 μg/ml) and gentamicin (50 μg/ml). The fore and hind limb buds of embryos were collected under a dissecting microscope. After all limb buds were collected, they were transferred into 0.25% trypsin-0.1% EDTA and incubated at 37 °C for 15 min with gentle shaking (approximately 80 rpm) in water bath. Cells released from the first digestion were collected and the equal volume of DMEM/F12 medium with 10% FBS was added to inactivate trypsin. The cells from the second and third digestions were treated as the same as the first-time digestion. The mixture of dissociated limbs was filtered through a 40-μm pore size cell strainer. The single cell suspension was centrifuged at 300 g and 4 °C for 10 min. Cells were resuspended at a density of 2×10^7 cells/ml in DMEM/F12 medium containing 10% FBS. 3×10^5 cells in 15 μl of medium were placed in the center of a 24-well plate and incubated in 5% CO_2 at 37 °C. After 1 h, 0.5 ml of culture medium was gently added to each well. ABL or other reagents were added to micromass cultures on the same day. Medium, ABL and other reagents were changed every other day.

For generation of primary chondrocyte cultures, femoral heads, femoral condyles and tibial plateaus were collected using a dissecting microscope from 2-3-day-old C57BL/6 mice and digested three times with 3 mg/ml collagenase D for 1 h at 37 °C with gentle agitation. Cells released from the first digestion were discarded, and cells from the second and third digestions were grown in DMEM medium supplemented with 10% fetal bovine serum, 100 units/ml penicillin, and 100 μg/ml streptomycin. After trypsinization of the confluent cells, chondrocytes were used for the experiments [16].

2.3. Alcian blue staining

Alcian blue staining was conducted by applying a solution of 0.5% Alcian blue (pH1.0) for 0.5 h at room temperature, and washed with 0.5 N hydrochloric acid. For quantification of cartilage-like nodule formation, Alcian blue-positive colonies were visualized using EVOS FL Auto Cell Imaging System (Invitrogen) and counted manually under a phase-contrast microscope. To quantify the staining intensity, the wells in the stained culture plates were extracted with 6 M guanidine hydrochloride for 10 h at room temperature. The absorbance of the extracted dye was measured using a spectrophotometer at 620 nm [17].

2.4. mRNA abundance quantification

Total RNA from mesenchymal cells in micromass cultures was extracted with TRIzol, treated with DNase, converted to cDNA, and subjected to quantitative real time PCR, and primer sequences of PTH1R and β-actin was listed as previously described [18].

2.5. Preparation of paraffin sections

Mesenchymal limb bud cells placed in micromass cultures are differentiated into chondrocytes that secrete abundant matrix to form cartilaginous tissue. Pellet cultures were removed manually on days 7, 14, and 21, fixed in 4% paraformaldehyde, embedded in paraffin, and sectioned [19].

2.6. Immunofluorescence assay

The deparaffinized sections were conducted for antigen retrieval and then permeabilized with 0.1% Triton X-100 as previously described [18]. Anti-collagen type X (Col X) antibody diluted 1:250 in blocking buffer was applied to the specimens at room temperature for 1 h. Alexa Fluor 488-tagged goat anti-rabbit second antibody diluted 1:500 was applied under the same conditions as the primary antibody. Nuclear staining was performed with DRAQ5.

2.7. Apoptosis assay

Chondrocyte apoptosis in deparaffinized sections was measured by terminal deoxynucleotidyl transferase dUTP nick end labeling (TUNEL) assay using In Situ Apoptosis Detection kit following the supplier's instructions. Normal nuclei were counterstained with methyl green.

2.8. Matrix mineralization assay by von Kossa staining

The deparaffinized sections were incubated with 5% fresh silver nitrate solution under UV light. Mineralized nodules were seen as dark brown to black spots. After unreacted silver was removed, the sections were counterstained with 1% eosin for 0.5 min to show cytoplasm staining [19].

2.9. Measurement of intracellular ROS

Primary mesenchymal cells in micromass cultures were placed in the center of a 24-well plate. After four days, the cultures were changed to serum-free medium for 2 h and then loaded with 2′,7′-dichlorofluorescin diacetate (DCF-DA, 150 μM), a parent nonfluorescent compound, for 10 min. The moicromass cultures were washed with serum-free medium and treated with ABL (10 nM), PTH(1–34) (10 nM), NAC (1 mM) or vehicle for 2 h. The ABL and other reagents were then removed and the DCF fluorescence in 0.25 ml of calcium and magnesium phosphate-buffered saline was visualized with EVOS FL Auto Cell Imaging System and intracellular fluorescence intensity was detected by a plate reader (Synergy-2) using an excitation wavelength of 485 nm and an emission wavelength of 520 nm [15,21]. Fluorescence intensity is presented as actual meter reading divided by 1000.

2.10. cAMP formation and measurement

cAMP measurements were performed in primary articular chondrocytes. The cells were treated with vehicle, ABL or PTH(1-34) in the presence of phosphodiesterase inhibitor 3-isobutyl-1-methylxanthine (1 mM) for 15 min cAMP formation was detected using the cyclic AMP Direct EIA Kit (Arbor Assays) following the supplier's instructions. The samples were analyzed by using a cAMP standard curve [20].

2.11. Intracellular calcium assay

Primary articular chondrocytes were loaded with 2 μM Fluo-4 AM according to the manufacturer's protocol. ABL, PTH(1-34) or vehicle was added by an automated pipetting system in triplicate, and the 525-nm signals were generated by excitation at 485 nm with a Flex Station II (Molecular Devices, Sunnyvale, CA) as previously reported [20].

2.12. Statistical analysis

The data are presented as the means ± SEM of triplicate measurements. In the figures, *n* indicates the number of independent experiments. Statistical analysis between control and treated groups was performed using Student's *t*-test. Multiple comparisons were evaluated by one-way or two-way analysis of variance followed by Bonferroni's posttest (Prism; GraphPad). p values < 0.05 were assumed to be significant.

3. Results

3.1. Mouse limb bud mesenchymal stem cells in micromass culture spontaneously undergo chondrogenesis, chondrocyte hypertrophy, apoptosis and terminal differentiation

The cell model of mouse limb bud mesenchymal stem cells in micromass culture was used to examine different stages of mesenchymal cell differentiation. The day of initial drop culture was considered as day 0. The cartilage nodules appeared by day 2 and the increase of cartilage nodule formation overtime was confirmed by Alcian blue staining for proteoglycan formation in extracellular matrix (Fig. 1A). The cartilaginous tissue progressively thickened and was manually removed for histologic evaluation. The expression of Col X level, a chondrocyte hypertrophic marker, was not detected on day 7, but increased on day 14 (Fig. 1B). Chondrocyte apoptosis did not appear on day 7, but occurred on day 21, as evidenced by induction of TUNEL-positive cells (Fig. 1C). The matrix calcification (the terminal chondrocyte differentiation) was detected and mineralized area occurred on day 21 (Fig. 1D). Collectively, chondrogenic differentiation in high-density micromass cultures undergoes an orderly series of changes, which mimics the endochondral ossification during growth plate development *in vivo* [11,12].

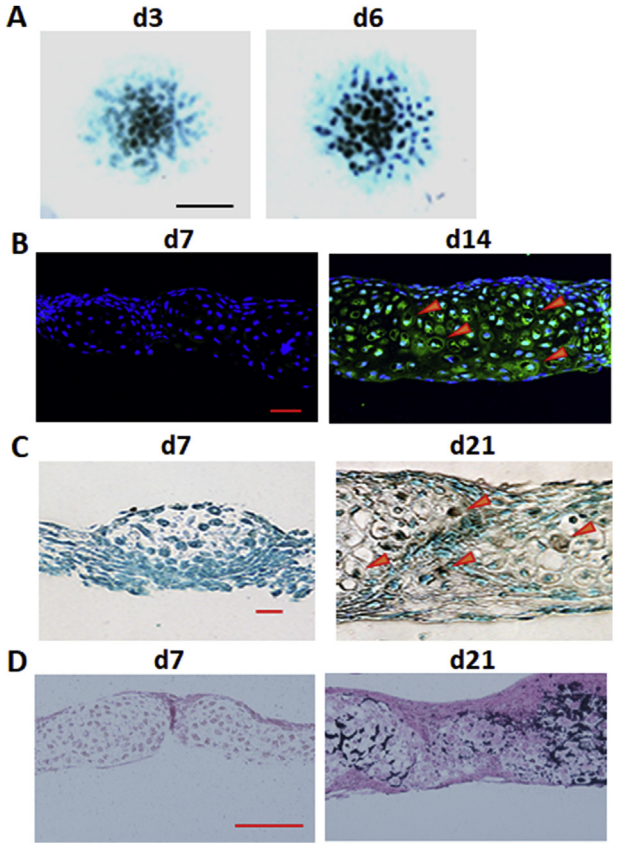

Fig. 1. Mouse limb bud mesenchymal stem cells in micromass culture spontaneously undergo the entire process of differentiation. Representative of three independent experiments performed with similar results. A. Alcian blue staining on days 3 and 6. Bar: 2 mm. B. Col X expression by fluorescent staining on days 7 and 14 was shown in green and nuclear staining was shown in blue. Bar, 100 μm. Arrowheads indicate hypertrophic cells. C. Chondrocyte apoptosis occurs on day 21. Arrowheads show dark brown TUNEL-positive apoptotic cells. Normal nuclei are light green in color (methyl green counterstain). Bar: 20 μm. D. Cartilaginous tissue were stained with silver nitrate solution under UV light. Mineralized nodules were seen as dark brown to black spots. Bar, 100 μm. (For interpretation of the references to color in this figure legend, the reader is referred to the Web version of this article.)

3.2. ABL has biological activity similar to that of PTH(1-34) in enhancing mesenchymal stem cell chondrogenic differentiation

Several lines of evidence have demonstrated that PTH(1-34) and PTHrP(1-36) have effect to stimulate chondrogenic differentiation [17,22,23]. PTH1R activation elicits $G\alpha_s$/cAMP and $G\alpha_q$/phospholipase C (PLC) pathways. We compared the effects of PTH(1-34) and ABL on cAMP formation and intracellular calcium $[Ca^{2+}]_i$, an index of PLC activity, in primary articular chondrocytes. ABL (10 nM) had a trend towards an increase of more cAMP formation compared with effect of 10 nM PTH(1-34). PLC activity was undetectable with 10 nM of ABL or PTH(1-34) treatment (data not shown), however, 100 nM PTH(1-34) and ABL had similar effects on stimulating PLC activity (Fig. 2A). Chondrogenesis is the initial stage of mesenchymal stem cell differentiation in micromass cultures. Exposure of cells to PTH(1-34) or ABL was for the first 6 h of each 48 h cycle. Both 10 nM of PTH(1-34) and ABL treatment for 4 days significantly

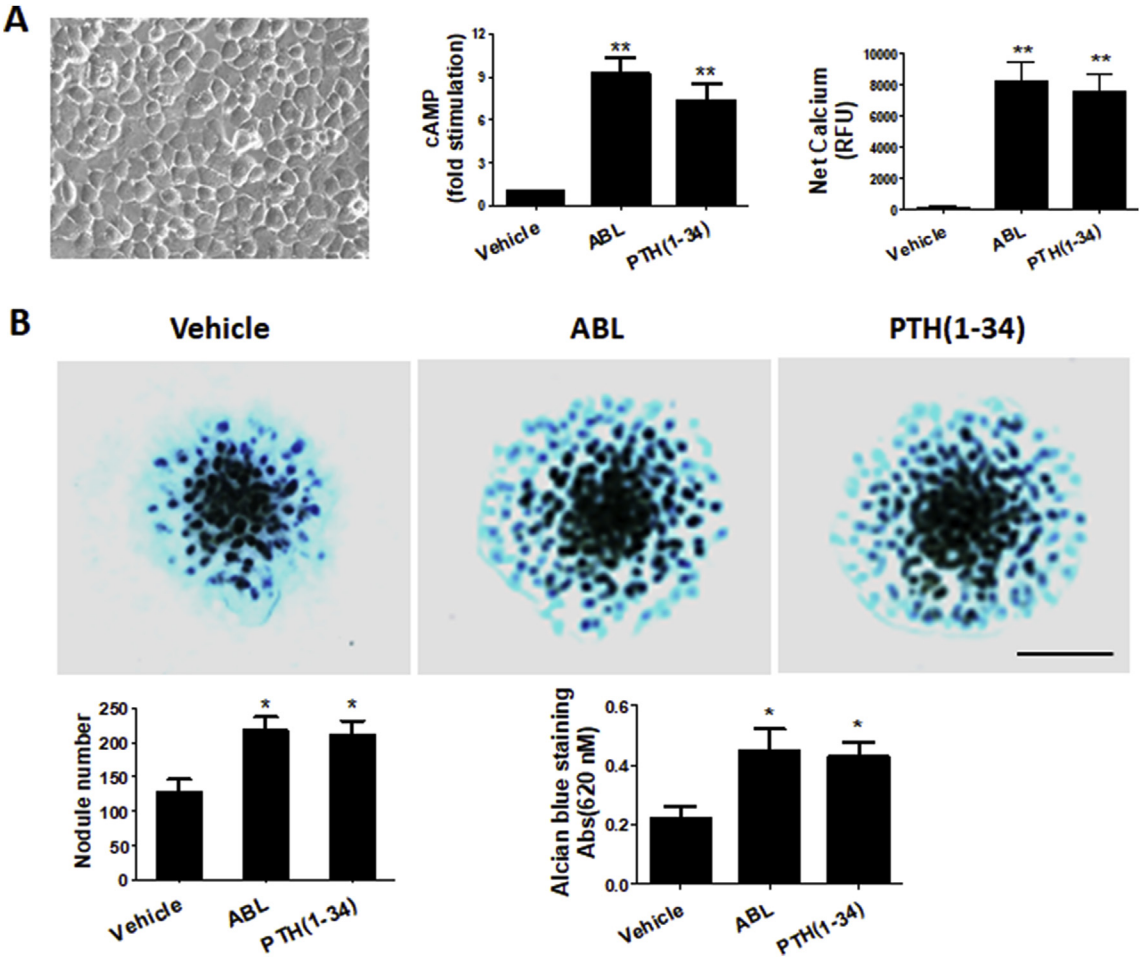

Fig. 2. ABL enhances mesenchymal stem cell chondrogenic differentiation. A. The confluence of mouse primary articular chondrocytes from newborn mice is shown in left panel. ABL and PTH(1-34) stimulated cAMP formation (middle panel) and intracellular calcium (right panel) in primary articular chondrocytes. B. Representative of three independent experiments performed with similar results for Alcian blue staining on day 5. Bar: 2 mm (upper panel). Quantitative assessment of cartilage nodule number (lower, left) and intensity of Alcian blue staining (lower right). Data are presented as mean ± SEM. n = 4. *, $p < 0.05$, **, $p < 0.01$, *versus* vehicle control. (For interpretation of the references to color in this figure legend, the reader is referred to the Web version of this article.)

increased cartilage nodule number and Alcian blue staining intensity (Fig. 2B).

3.3. *N-acetyl-L-cysteine (NAC) enhances increases cartilage nodule formation*

Oxidative stress plays an important role in causing mesenchymal cell death during isolation and expansion process [13]. NAC, which exerts protective effects on oxidative damages, stimulates osteoblastic differentiation of mouse calvarial cells [24]. We asked whether NAC also stimulated chondrogenic differentiation. NAC (1 mM), N-Acetyl-L-alanine (NAA) (1 mM), a negative control, or vehicle was added to micromass cultures for 4 days. The medium, NAC or NAA was changed every two days. Data in Fig. 3A showed that NAC but not NAA enhanced chondrogenic differentiation, as evidenced by increase of cartilage nodule number (Fig. 3B) and Alcian blue staining intensity (Fig. 3C).

3.4. *ABL inhibits ROS production in limb bud-derived mesenchymal cells*

Both PTH(1-34) and PTHrP(1-36) have anti-oxidant effects [14,15]. Since ABL and NAC enhance chondrogenesis, we hypothesize that limb bud-derived mesenchymal cells in micromass cultures produce ROS and ABL-stimulated chondrogenesis is involved in its inhibition of ROS production. To test this idea, we examined the effects of ABL, PTH(1-34) and NAC on intracellular ROS production in limb bud-derived mesenchymal cells on day 5. Our data showed that DCF fluorescence was visualized only within the cartilage nodules (Fig. 4A). NAC (1 mM), 10 nM ABL or PTH(1-34) treatment for 2 h significantly reduced ROS generation, as evidenced by decrease of fluorescence intensity (Fig. 4A and B). We further found that *PTH1R* gene expression increased gradually over a 5-day time period (Fig. 4C). ABL and PTH(1-34) but not NAC increased *PTH1R* gene expression, suggesting ABL and NAC inhibit ROS production through different mechanisms.

4. Discussion

It is necessary to manipulate mesenchymal cell to resist severe stresses, and targeting oxidative stress is one of effective strategies for prevention and treatment of OA [25,26]. To the best of our knowledge, this is the first report showing ABL-induced chondrogenesis is involved in inhibiting intracellular ROS production.

To elucidate the mechanism by which ABL affects chondrocyte differentiation, we first need to choose *in vitro* model that mimics *in vivo* chondrogenic development. Over the past decades, many *in vitro* models have been established to study chondrogenesis and

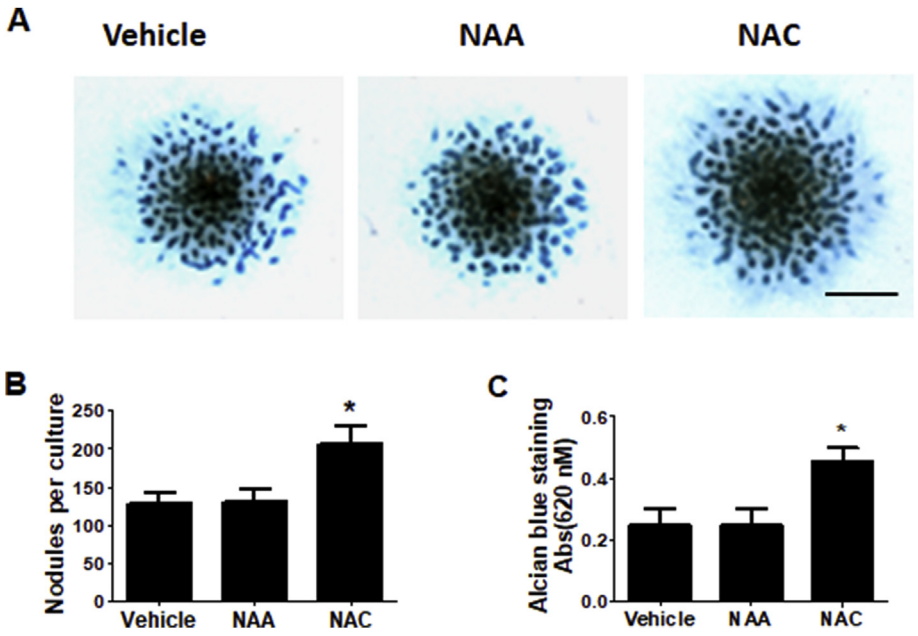

Fig. 3. NAC promotes chondrogenic differentiation. A. NAC (1 mM) but not NAA (1 mM) stimulates cartilage nodule formation. Representative of three independent experiments performed with similar results for Alcian blue staining on day 5. Bar: 2 mm. B. Quantitative assessment of cartilage nodule number. C. Intensity of Alcian blue staining. Data are presented as mean ± SEM. n = 4. *, $p < 0.05$, *versus* vehicle control. (For interpretation of the references to color in this figure legend, the reader is referred to the Web version of this article.)

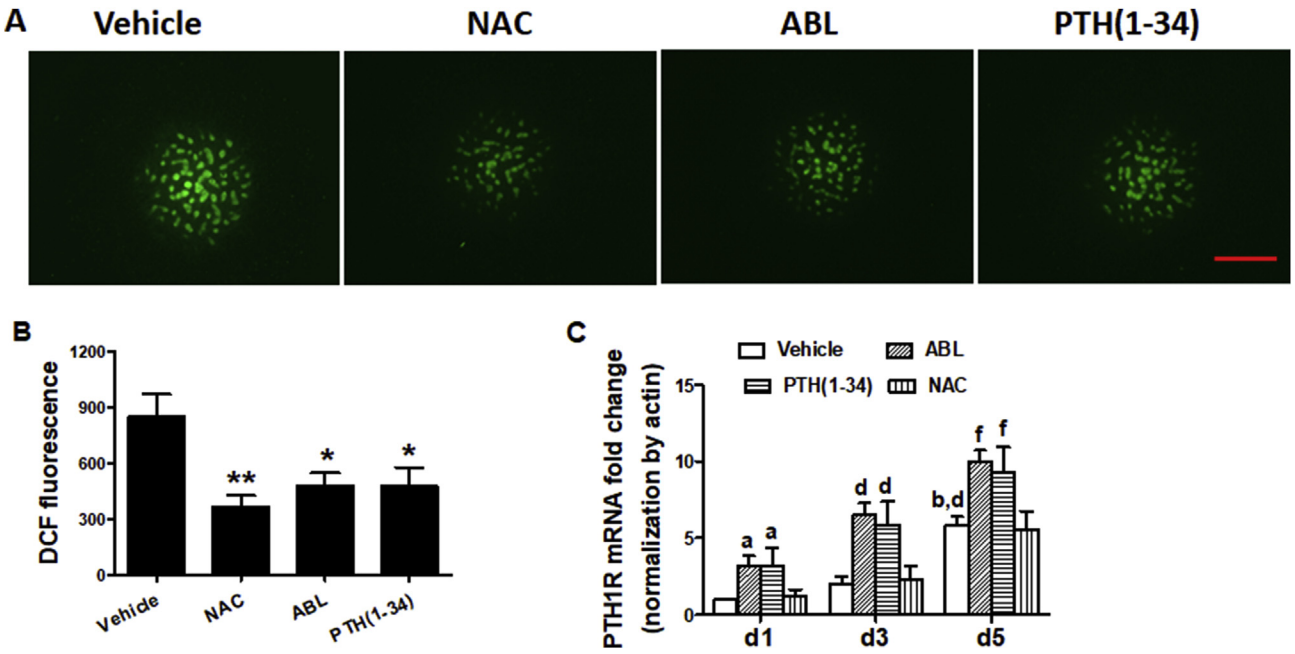

Fig. 4. ABL inhibits ROS production in limb bud-derived mesenchymal cells. Mesenchymal stem cells (3×10^5 cells in 15 μl) were placed in the center of 24-well plate on day 0. On day 5, the cultures were serum-starved for 2 h and then loaded with DCF-DA (150 μM) for 10 min. After loading, ABL (10 nM), PTH(1-34) (10 nM), NAC (1 mM) or vehicle was added to the cultures for 2 h. A. The fluorescence imaging was recorded using EVOS FL Auto Cell Imaging System and representative of three independent experiments performed with similar results is shown. Bar: 1 mm. B. DCF fluorescence intensity was measured. n = 5. *, $p < 0.05$, **, $p < 0.01$, *versus* vehicle control. C. Mesenchymal cells in micromass were treated with 10 nM ABL, 10 nM PTH(1-34), 1 mM NAC, or vehicle from day 0 to day 4. The mRNA expression of *PTH1R* was measured on days 1, 3, and 5 by quantitative real time PCR. The data are presented as fold change and summarized as the means ± SEM. n = 4. a, $p < 0.05$, b, $p < 0.01$ *versus* vehicle on d1; c, $p < 0.05$, d, $p < 0.01$ *versus* vehicle on d3; e, $p < 0.05$, f, $p < 0.01$ *versus* vehicle on d5.

chondrocyte hypertrophy. These models include cell lines of mesenchymal cells, embryonic limb bud-derived mesenchymal cells, growth plate chondrocytes, and bone marrow-derived mesenchymal cells [12,27]. The entire process of endochondral ossification requires a series of well-orchestrated events. The initial condensation of mesenchymal cells is a prerequisite to their subsequent differentiation. Mouse limb bud mesenchymal cells in high-density micromass cultures recapitulate events occurred during endochondral ossification. Thus, mouse embryonic limb bud-derived mesenchymal cells in micromass cultures were used to examine effect of ABL on the chondrogenic differentiation.

Oxidative stress negatively or positively modulates

mesenchymal stem cell differentiation due to exposure to different magnitudes of ROS [26,28]. To understand the molecular mechanisms of ABL on chondrogenic differentiation, we investigated whether endogenous ROS production in mircomass cultures affected mesenchymal stem cell differentiation to chondrocytes. Our data show that NAC significantly enhances chondrogenesis. We found that mesenchymal stem cells in micromass culture spontaneously produced ROS. Both NAC and ABL promoted chondrogenesis by reducing ROS production. Our data further show that ABL but not NAC increases *PTH1P* mRNA expression, suggesting ABL effect on inhibition of ROS production is mediated by PTH1R-dependent signaling pathway. Sequential proliferation, hypertrophy and maturation of chondrocytes in embryonic limb bud-derived micromass cultures are tightly regulated by cell signaling [12]. PTHrP maintains cartilage development and attenuates chondrocyte hypertrophy through $G\alpha_s$/cAMP signaling pathway by interacting with Indian hedgehog to modulate transcriptional activity of SRY-box9 (SOX9) and runt-related transcription factors (Runx), whereas $G\alpha_q$/PLC activation appears to increase ROS production [29]. Recently, it was reported that chondrogenesis induced by PTH(1-34) in mesenchymal stem cells is mediated by Runx1 via the activation of cAMP/PKA pathway [17]. Future investigations will be needed to assess which PTH1R signaling pathways mediate ABL effect on reducing ROS production during chondrogenic differentiation. ROS are free radicals containing various oxidant molecules and further studies will be necessary to determine what specific oxidants are produced by mesenchymal cells in micromass cultures.

In conclusion, mesenchymal stem cells are becoming a promising cell source for cartilage regeneration. However, these cells are poor survival after transplantation and acquire hypertrophic properties during chondrogenic induction. The present study has demonstrated that ABL-stimulated chondrogenesis is related to its reducing ROS production in mesenchymal stem cells. In addition, PTHrP exhibits potent inhibition of chondrocyte hypertrophy. ABL has been used for osteoporosis therapy. Our findings support that ABL may be considered as a novel means for OA cartilage defect regeneration.

Conflicts of interest

The authors have no conflict of interest to disclose.

Transparency document

Transparency document related to this article can be found online at https://doi.org/10.1016/j.bbrc.2019.01.049.

Funding sources

This work was supported in part by the U.S. Department of Defense Grant W81XWH-16-1-0325 (to B. W.).

References

[1] R.F. Loeser, Aging processes and the development of osteoarthritis, Curr. Opin. Rheumatol. 25 (2013) 108–113.
[2] A. Goldberg, K. Mitchell, J. Soans, L. Kim, R. Zaidi, The use of mesenchymal stem cells for cartilage repair and regeneration: a systematic review, J. Orthop. Surg. Res. 12 (2017) 39.
[3] N.K. Dubey, V.K. Mishra, R. Dubey, S. Syed-Abdul, J.R. Wang, P.D. Wang, W.P. Deng, Combating osteoarthritis through stem cell therapies by rejuvenating cartilage: a review, Stem Cell. Int. 2018 (2018), 5421019.
[4] T.E. Robey, M.K. Saiget, H. Reinecke, C.E. Murry, Systems approaches to preventing transplanted cell death in cardiac repair, J. Mol. Cell. Cardiol. 45 (2008) 567–581.
[5] M. Lo Monaco, G. Merckx, J. Ratajczak, P. Gervois, P. Hilkens, P. Clegg, A. Bronckaers, J.M. Vandeweerd, I. Lambrichts, Stem cells for cartilage repair: preclinical studies and insights in translational animal models and outcome measures, Stem Cell. Int. 2018 (2018), 9079538.
[6] E.R. Sampson, M.J. Hilton, Y. Tian, D. Chen, E.M. Schwarz, R.A. Mooney, S.V. Bukata, R.J. O'Keefe, H. Awad, J.E. Puzas, R.N. Rosier, M.J. Zuscik, Teriparatide as a chondroregenerative therapy for injury-induced osteoarthritis, Sci. Transl. Med. 3 (2011) 101–193.
[7] J.P. Vilardaga, G. Romero, P.A. Friedman, T.J. Gardella, Molecular basis of parathyroid hormone receptor signaling and trafficking: a family B GPCR paradigm, Cell. Mol. Life Sci. 68 (2011) 1–13.
[8] E. Schipani, B. Lanske, J. Hunzelman, A. Luz, C.S. Kovacs, K. Lee, A. Pirro, H.M. Kronenberg, H. Juppner, Targeted expression of constitutively active receptors for parathyroid hormone and parathyroid hormone-related peptide delays endochondral bone formation and rescues mice that lack parathyroid hormone-related peptide, Proc. Natl. Acad. Sci. U. S. A. 94 (1997) 13689–13694.
[9] C. Macica, G. Liang, A. Nasiri, A.E. Broadus, Genetic evidence of the regulatory role of parathyroid hormone-related protein in articular chondrocyte maintenance in an experimental mouse model, Arthritis Rheum. 63 (2011) 3333–3343.
[10] M. Bernhardsson, P. Aspenberg, Abaloparatide versus teriparatide: a head to head comparison of effects on fracture healing in mouse models, Acta Orthop. (2018) 1–6.
[11] E.G.J. Ripmeester, U.T. Timur, M.M.J. Caron, T.J.M. Welting, Recent insights into the contribution of the changing hypertrophic chondrocyte phenotype in the development and progression of osteoarthritis, Front Bioeng. Biotechnol. 6 (2018) 18.
[12] X. Zhang, N. Ziran, J.J. Goater, E.M. Schwarz, J.E. Puzas, R.N. Rosier, M. Zuscik, H. Drissi, R.J. O'Keefe, Primary murine limb bud mesenchymal cells in long-term culture complete chondrocyte differentiation: TGF-beta delays hypertrophy and PGE2 inhibits terminal differentiation, Bone 34 (2004) 809–817.
[13] M. Mohammadzadeh, R. Halabian, A. Gharehbaghian, N. Amirizadeh, A. Jahanian-Najafabadi, A.M. Roushandeh, M.H. Roudkenar, Nrf-2 overexpression in mesenchymal stem cells reduces oxidative stress-induced apoptosis and cytotoxicity, Cell Stress Chaperones 17 (2012) 553–565.
[14] R.L. Jilka, M. Almeida, E. Ambrogini, L. Han, P.K. Roberson, R.S. Weinstein, S.C. Manolagas, Decreased oxidative stress and greater bone anabolism in the aged, when compared to the young, murine skeleton with parathyroid hormone administration, Aging Cell 9 (2010) 851–867.
[15] S. Portal-Nunez, J.A. Ardura, D. Lozano, I. Martinez de Toda, M. De la Fuente, G. Herrero-Beaumont, R. Largo, P. Esbrit, Parathyroid hormone-related protein exhibits antioxidant features in osteoblastic cells through its N-terminal and osteostatin domains, Bone Joint Res. 7 (2018) 58–68.
[16] M. Gosset, F. Berenbaum, S. Thirion, C. Jacques, Primary culture and phenotyping of murine chondrocytes, Nat. Protoc. 3 (2008) 1253–1260.
[17] J. Wang, X. Wang, J.D. Holz, T. Rutkowski, Y. Wang, Z. Zhu, Y. Dong, Runx1 is critical for PTH-induced onset of mesenchymal progenitor cell chondrogenic differentiation, PLoS One 8 (2013), e74255.
[18] B. Wang, Y. Yang, L. Liu, H.C. Blair, P.A. Friedman, NHERF1 regulation of PTH-dependent bimodal Pi transport in osteoblasts, Bone 52 (2013) 268–277.
[19] N. Schmitz, S. Laverty, V.B. Kraus, T. Aigner, Basic methods in histopathology of joint tissues, Osteoarthritis Cartilage 18 (Suppl 3) (2010) S113–S116.
[20] Y. Yang, H. Lei, Y.W. Qiang, B. Wang, Ixazomib enhances parathyroid hormone-induced beta-catenin/T-cell factor signaling by dissociating beta-catenin from the parathyroid hormone receptor, Mol. Biol. Cell 28 (2017) 1792–1803.
[21] C. Peiro, N. Lafuente, N. Matesanz, E. Cercas, J.L. Llergo, S. Vallejo, L. Rodriguez-Manas, C.F. Sanchez-Ferrer, High glucose induces cell death of cultured human aortic smooth muscle cells through the formation of hydrogen peroxide, Br. J. Pharmacol. 133 (2001) 967–974.
[22] J. Fischer, A. Aulmann, V. Dexheimer, T. Grossner, W. Richter, Intermittent PTHrP(1-34) exposure augments chondrogenesis and reduces hypertrophy of mesenchymal stromal cells, Stem Cell. Dev. 23 (2014) 2513–2523.
[23] Y.J. Kim, H.J. Kim, G.I. Im, PTHrP promotes chondrogenesis and suppresses hypertrophy from both bone marrow-derived and adipose tissue-derived MSCs, Biochem. Biophys. Res. Commun. 373 (2008) 104–108.
[24] J.H. Jun, S.H. Lee, H.B. Kwak, Z.H. Lee, S.B. Seo, K.M. Woo, H.M. Ryoo, G.S. Kim, J.H. Baek, N-acetylcysteine stimulates osteoblastic differentiation of mouse calvarial cells, J. Cell. Biochem. 103 (2008) 1246–1255.
[25] B. Poulet, F. Beier, Targeting oxidative stress to reduce osteoarthritis, Arthritis Res. Ther. 18 (2016) 32.
[26] P. Lepetsos, A.G. Papavassiliou, ROS/oxidative stress signaling in osteoarthritis, Biochim. Biophys. Acta 1862 (2016) 576–591.
[27] A.M. DeLise, E. Stringa, W.A. Woodward, M.A. Mello, R.S. Tuan, Embryonic limb mesenchyme micromass culture as an in vitro model for chondrogenesis and cartilage maturation, Methods Mol. Biol. 137 (2000) 359–375.
[28] L.B. Boyette, O.A. Creasey, L. Guzik, T. Lozito, R.S. Tuan, Human bone marrow-derived mesenchymal stem cells display enhanced clonogenicity but impaired differentiation with hypoxic preconditioning, Stem Cells Transl. Med. 3 (2014) 241–254.
[29] T. Inoguchi, T. Sonta, H. Tsubouchi, T. Etoh, M. Kakimoto, N. Sonoda, N. Sato, N. Sekiguchi, K. Kobayashi, H. Sumimoto, H. Utsumi, H. Nawata, Protein kinase C-dependent increase in reactive oxygen species (ROS) production in vascular tissues of diabetes: role of vascular NAD(P)H oxidase, J. Am. Soc. Nephrol. 14 (2003) S227–S232.